SDU
University of Southern Denmark

The Late Cretaceous Western Interior Seaway as a model for oxygenation change in epicontinental restricted basins

Lowery, Christopher M.; Leckie, R. Mark; Bryant, Raquel; Elderbak, Khalifa; Parker, Amanda; Polyak, Desiree E.; Schmidt, Maxine; Snoeyenbos-West, Oona; Sterzinar, Erica

Published in:
Earth-Science Reviews

DOI:
10.1016/j.earscirev.2017.12.001

Publication date:
2018

Document version:
Accepted manuscript

Document license:
CC BY-NC-ND

Citation for pulished version (APA):
Lowery, C. M., Leckie, R. M., Bryant, R., Elderbak, K., Parker, A., Polyak, D. E., Schmidt, M., Snoeyenbos-West, O., & Sterzinar, E. (2018). The Late Cretaceous Western Interior Seaway as a model for oxygenation change in epicontinental restricted basins. *Earth-Science Reviews*, *177*, 545-564. https://doi.org/10.1016/j.earscirev.2017.12.001

Go to publication entry in University of Southern Denmark's Research Portal

Terms of use
This work is brought to you by the University of Southern Denmark.
Unless otherwise specified it has been shared according to the terms for self-archiving.
If no other license is stated, these terms apply:

- You may download this work for personal use only.
- You may not further distribute the material or use it for any profit-making activity or commercial gain
- You may freely distribute the URL identifying this open access version

If you believe that this document breaches copyright please contact us providing details and we will investigate your claim.
Please direct all enquiries to puresupport@bib.sdu.dk

Download date: 06. Nov. 2026

The Late Cretaceous Western Interior Seaway as a Model for Oxygenation Change in Epicontinental Restricted Basins

Christopher M. Lowery

University of Texas Institute for Geophysics

10100 Burnet Rd., Austin, TX 78758

R. Mark Leckie

University of Massachusetts, Amherst

600 N. Pleasant St., Amherst, MA 01003

Raquel Bryant

University of Massachusetts, Amherst

600 N. Pleasant St., Amherst, MA 01003

Khalifa Elderbak

ALS Oil and Gas

Houston, TX

6510 Guhn Rd, Houston, TX 77040

Amanda Parker

University of Massachusetts, Amherst

600 N. Pleasant St., Amherst, MA 01003

Desiree E. Polyak

U.S. Geological Survey- National Minerals Information Center

989 National Center, Reston, VA 20192

Maxine Schmidt

University of Massachusetts, Amherst

600 N. Pleasant St., Amherst, MA 01003

Oona Snoeyenbos-West

University of Massachusetts, Amherst

600 N. Pleasant St., Amherst, MA 01003

Erica Sterzinar

Langan Engineering and Environmental Services, Inc.

300 Kimball Dr., Parsippany, NJ 07054

KEYWORDS: Ocean Deoxygenation, Cretaceous, OAE2, OAE3, Foraminifera, Western Interior Sea

ABSTRACT

Deoxygenation is a critical problem facing the ocean as the world warms, and has the potential to effect coastal upwelling zones, shelf areas influenced by high runoff and nutrification, and restricted and semi-restricted basins. The mechanisms that drive deoxygenation in these diverse environments are still not fully understood, in part because the modern record of redox change is short and anoxia is still relatively rare in the modern ocean. Here, we address this problem of scale by studying deoxygenation in the geologic past. We summarize decades of individual studies of benthic foraminifera to generate a record of bottom water oxygen change in the Cretaceous Western Interior Sea (WIS) of North America over ~13 myr (Cenomanian-Campanian), spanning two major sea level cycles. The WIS was prone to major changes in dissolved oxygen content throughout its long history, sometimes directly antiphase to trends in the global ocean.

Presented as maps, our data show that bottom water oxygen within the WIS was controlled by a combination of water mass source and mixing moderated by sea level and basin restriction. Areas flooded by cool Boreal (northern-sourced) waters in the northern and western parts of the seaway were better oxygenated than the eastern and southern portions of the seaway, which were flooded by warmer Tethyan (southern-sourced) waters. Beyond east-west differences explained by water mass, the entire seaway was better oxygenated during periods of transgression, and more poorly oxygenated to anoxic during periods of peak transgression/highstand and regression. We suggest that this pattern was due to the formation and downwelling of Western Interior Intermediate Water by the mixing of Tethyan and Boreal waters. During transgressions, an increasing volume of these watermasses entered the

seaway, mixed, and downwelled well-oxygenated surface water to the seafloor. During late transgression/highstand, partial stratification and the encroachment of low oxygen waters from the open ocean caused dissolved oxygen levels to drop at the seafloor, but continued downwelling prevented anoxia. During the subsequent regression, a decline in the volume of outside watermasses entering the seaway caused a reduction in mixing and weakened downwelling which led to stratification and seafloor anoxia.

As a model for other semi-restricted basins, the trends observed in the WIS show that local changes in relative sea level, mixing, and circulation are critical in controlling oceanic deoxygenation in these environments, in clear contrast to continental margins impinged by oxygen minimum zones, like the contemporaneous Demerara Rise in the southern Caribbean. Although the WIS is larger than most semi-restricted basins, it is characterized by quasi-estuarine circulation driving the interaction of normal marine and brackish watermasses, and thus serves a model for similar shallow epicontinental basins of any size. Understanding how these processes vary in different environments is key to predicting susceptibility of regional water bodies to deoxygenation in the future with a warming world.

1. Introduction

Oceanic deoxygenation is a critical process to understand as the world continues to warm. A combination of the diminished capacity of warming water to hold dissolved gases and rising sea level will cause a decline in dissolved oxygen content in the modern world ocean (e.g., Oschilies et al., 2008), a phenomenon that is already being observed (Stramma et al., 2010; Ito et al., 2017). Interestingly, most of the modern negative trend in dissolved oxygen is attributed to apparent oxygen utilization by organisms in the water column, rather than thermal effects (Ito et al., 2017), and is therefore greater than predicted. The reasons for this are not fully understood, highlighting the need for further studies of the ways in which ocean circulation, mixing, and biogeochemical cycles can drive deoxygenation.

Deoxygenation in the modern ocean is caused by the eutrophication of semi-restricted basins like the Baltic Sea, Chesapeake Bay, and Black Sea (e.g., Diaz and Rosenberg, 2008), and the expansion of oxygen minimum zones in coastal upwelling regions (e.g., Helly and Levin, 2004). Unfortunately, the modern history of observations in these regions is limited. Indeed, in many basins, anoxia due to eutrophication has only been established in the last 50 years; for example, dead zones in the northern Gulf of Mexico didn't appear until the 1970s (Rabalais and Turner, 2001). In order to study the formation of anoxic conditions due to changing climate and determine their long-term impact on ecosystems it is necessary to look to the geologic past. One of the best-known intervals of ocean deoxygenation during the Phanerozoic Eon is the Cretaceous Period, which was characterized by short-lived intervals of widespread anoxia and black shale deposition known as Oceanic Anoxic Events (OAEs; Schlanger and Jenkyns, 1976; Jenkyns, 2010).

Although OAEs are typically considered to be periods of widespread anoxia, there are many localities which remained oxic during these events, and often local black shales and anoxic conditions were diachronous (Tsikos, 2004). A good example of increasing oxygen during OAEs is in the Western Interior Sea (WIS) of North America, a semi-restricted basin similar to many modern anoxic environments, where the well-studied Cenomanian-Turonian OAE2 is associated with a shift from anoxic to well-oxygenated bottom waters at the onset of OAE2. More broadly, anoxia and organic matter enrichment in the WIS often behave in anti-phase to what would be expected based on models for black shale development in restricted environments. Generally, sea level transgressions are associated with anoxia and black shale deposition in shelf and shallow sea environments, as rising sea level causes condensation of sediments at the seafloor and stratification of the water column, and expanding shelves and inland seas trap more terrigenous organic matter (Arthur and Sageman, 1994; 2005). However, part of the transgressive phases of the two largest sea level cycles in the WIS are associated with increased oxygen and decreased organic matter preservation (Eicher and Diner, 1985; Pratt et al., 1985; Sageman,

1989; Arthur and Sageman, 1994; Leckie et al., 1998; Svarda, 1998a; Elderbak and Leckie, 2016; Lowery et al., 2017a). These observations stand in direct contrast to both the global trend (especially during OAE2), and the model for anoxia and organic matter enrichment on open shelf environments in general, and suggest a more complex driver.

Understanding the cause(s) of this heterogeneity is essential for understanding the processes that drive deoxygenation on continental margins and in shallow seas. Continental margins and inland seas tend to be more productive than the open ocean (e.g., Diaz and Rosenberg, 2008, and references therein) and more prone to anoxia. During the high sea levels of the Cretaceous, flooded continental crust made up as much as ~17% of the ocean by area, according to ocean volume and sea level estimates (Müller et al., 2008; Kominz et al., 2008). These processes may have direct implications for modern basins with semi-enclosed morphologies and quasi-estuarine circulation.

Black shale deposition and the development of anoxia are the result of a combination of several factors, including enhanced primary production driving eutrophication, changes in oceanographic conditions resulting in enhanced preservation potential of organic matter under basically constant organic matter flux, decreased oxygen exposure time of organic carbon in sediments and/or the water column, and reduced dilution of organic matter by high sedimentary flux (e.g., Pedersen and Calvert, 1990, Hartnett et al., 1998; Sageman and Lyons, 2003; Sageman et al., 2014). Although anoxic events like OAE2 are the product of globally enhanced productivity (see review by Jenkyns, 2010), local deoxygenation and black shale deposition are always inherently local processes. In the WIS, geochemical studies of sedimentary organic matter (e.g., Meyers et al., 2001, 2005; Tessin et al., 2015, 2016) and nannofossil paleoproductivity indicators (Corbett and Watkins, 2013) indicate that organic matter preservation is largely due to changes in preservation potential rather than an increase in productivity. Intervals of high sedimentary organic matter content are generally associated with late transgression and highstand in the WIS (sea level trends commonly associated with black shale deposition; Arthur et

al., 1987; Wignall, 1991, Arthur and Sageman, 2005), which allowed the incursion of a low oxygen water mass, decreased dilution by terrigenous material, and, according to some, stagnation (Arthur and Sageman, 2005).

The WIS contains a wealth of data paired with excellent chronostratigraphic control, which together provide a unique opportunity to study long-term trends in paleoredox change in deep time. The seaway records five successive high-order sea level cycles that flooded a foreland basin from the Canadian Arctic to the Gulf of Mexico throughout the Cretaceous (Kauffman, 1984; Kauffman and Caldwell, 1993). Each of these cycles is exposed in countless outcrops along the entire expanse of the WIS, from Mexico to Canada and from Utah to Iowa, and as such the WIS has a long history of paleoenvironmental and paleoceanographic investigations (e.g., Gilbert, 1895; Eicher and Worstell, 1970; McNeil and Caldwell, 1981; Kauffman, 1984; Eicher and Diner, 1985; Caldwell et al., 1993; Kauffman and Caldwell, 1993; Pratt et al., 1993; Slingerland et al., 1996; Dean and Arthur, 1998; Leckie et al., 1998; Longman et al., 1998; Schröder-Adams et al., 1998; West et al., 1998; Meyers et al., 2001; Molenaar et al., 2002; Snow et al., 2005; Nielsen et al., 2008; Locklair et al., 2011; Sageman et al., 2014; Corbett et al., 2014; Elderbak et al., 2014; Schröder-Adams, 2014; Elderbak and Leckie, 2016; Kita et al., 2017; Lockshin et al., 2017; Lowery et al., 2017a) and a well-developed biostratigraphic zonation scheme based on ammonites and inoceramid bivalves (e.g., Merewether et al., 2011).

Benthic foraminifera are sensitive to a number of paleoenvironmental conditions, including salinity, food supply, pH, sea level, substrate, and turbidity, but in the WIS their distribution and abundance are primarily controlled by dissolved oxygen (Eicher and Worstell, 1970; Eicher and Diner, 1985; Leckie et al., 1998; West et al., 1998; Elderbak et al., 2014; Elderbak and Leckie, 2016; Lowery et al., 2017a). Here, we combine a large volume of data from 32 outcrop and core studies (Figure 1) to map the distribution of bottom water oxygen based on benthic foraminiferal abundance in the US Western Interior Sea for two cycles in the Late Cretaceous: the Cenomanian-Turonian Greenhorn Cycle and the

Turonian-Campanian Niobrara Cycle. These data are summarized in maps in ammonite-zone time slices which show how the distribution of dysoxic to anoxic bottom waters changes over time. We compare these trends to those observed at Demerara Rise, a coeval continental margin site influenced by upwelling and the impingement of an oxygen minimum zone (OMZ) on the seafloor. In doing so, we demonstrate how deoxygenation in Western Interior Sea and other shallow epicontinental seas, and the foraminiferal assemblages that characterized them, were fundamentally different from productive continental margins and the high-productivity benthic assemblages found there.

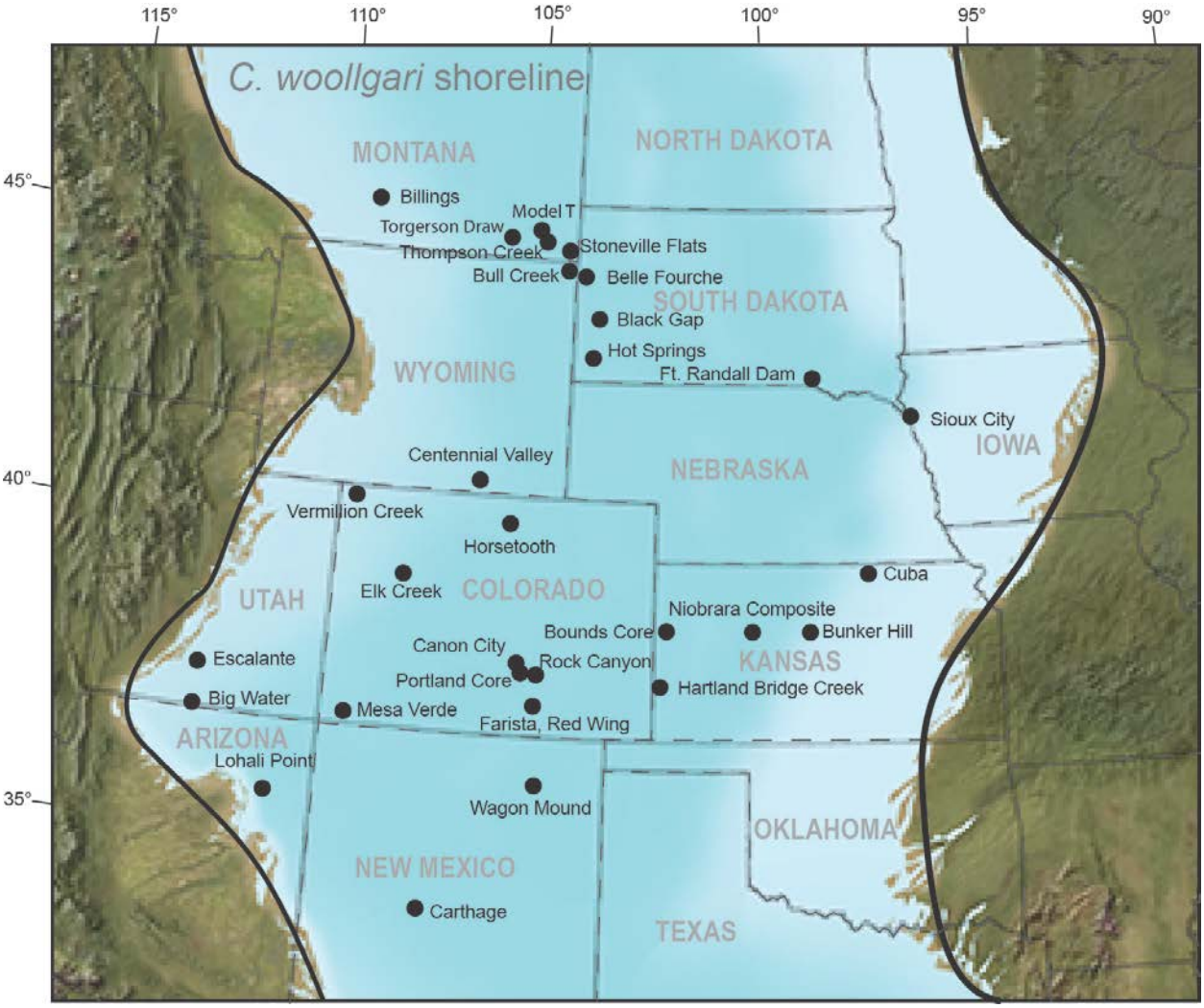


Figure 1. Location Map, showing the 32 total localities used in this study. Paleogeographic map representative of the middle Turonian *Colignoceras woollgari* Zone cropped from Blakey (2016).

2. The Western Interior Sea

Sea level change, North American climate, sediment input, and the varying influence of outside watermasses all strongly affected the oceanography of the Western Interior Sea. Paleoceanographers have long known that sea level, modulated by both eustasy and local tectonics, played an important role in the sedimentology and oxygenation history of the Western Interior Basin (Kauffman, 1984; Arthur and Sageman, 1994, 2005). The WIS had less than normal marine salinity during much of its history, as evidenced by the absence of many normal marine macroinvertebrates (e.g., echinoids, corals, bryozoans; Kauffman, 1984; Leckie et al., 1998). During periods of low sea level, a shallow carbonate platform in Texas acted as a sill, separating the WIS from the Gulf of Mexico (Arthur and Sageman, 2005; Lowery et al., 2014). During transgressions, rising sea level eventually overcame this sill and allowed warmer, normal marine water from the south to enter the seaway, bringing with it salinity-sensitive macro- and microfossils (Cobban and Reeside, 1952; Eicher and Worstell, 1970; Kaufmann, 1984; Eicher and Diner, 1985; Caldwell et al., 1993; Watkins et al., 1993; Leckie et al., 1998). These normal-marine organisms first colonized the deep central axis of the seaway, which was located along what is now the Front Range of the Rocky Mountains, from northeast New Mexico to southeast Wyoming. These transgressions also coincide with increased in carbonate accumulation, particularly on the eastern side of the basin; the western side, which was proximal to the Sevier Highlands, received higher terrigenous flux (Figure 2) (e.g., Kauffman, 1984).

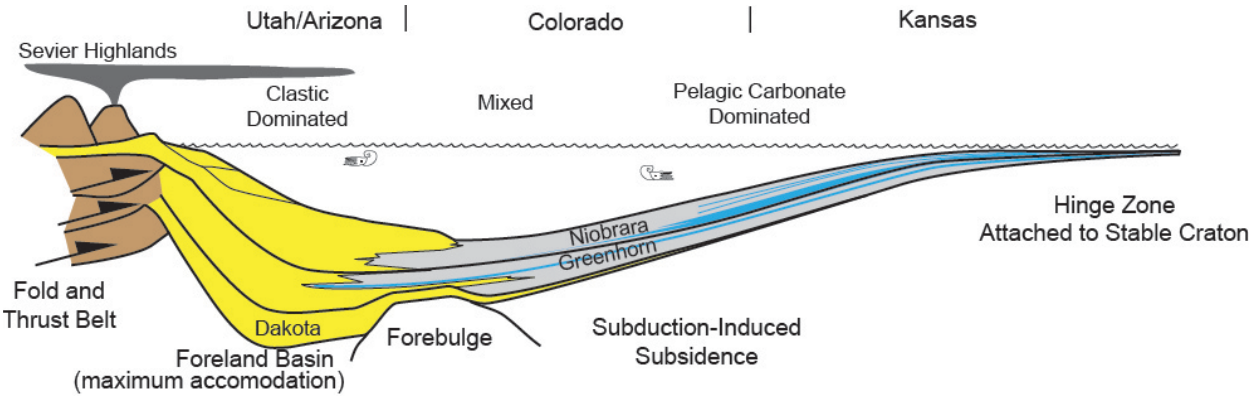


Figure 2. Idealized E-W cross section showing dominant sediment types and water depth trends with in the Western Interior Sea. Modified from Kauffman (1984).

2.1 Tectonics

The Western Interior Sea was a tectonically created foreland basin in which sea level and sediment accumulation were ultimately controlled by the high rates of tectonic activity along the western margin of North America during the Late Cretaceous (e.g., Gurnis, 1993). The subduction of the Farallon Plate beneath the North American Plate induced mantle flow driven dynamic subsidence that pulled the region below sea level, facilitated accommodation, and, along with eustasy, influenced stratigraphy and sea level cycles within the WIS (Pang and Nummendal, 1995; Liu and Nummendal, 2004; Liu et al., 2005, 2008, 2011, 2014). Superimposed on this mega-regional structural control, terrane accretion on the western margin of North America drove the Sevier Orogeny, which was characterized by a narrow fold and thrust belt along the western margin of the WIS (e.g., Armstrong, 1968; Schwartz and DeCelles, 1988). Thrust loading along the Sevier Mountains drove flexural subsidence which, combined with epiorogenic subsidence, formed a foreland basin along the western margin of the seaway (Pang and Nummendal, 1995; Liu et al., 2014). The thickest sediments in the WIS are found in foredeep of the foreland basin, due to proximity to the sediment source (i.e., the Sevier Highlands) and very high accommodation (e.g., Weimer, 1978; Ryer and Lovekin, 1986; White et al., 2002). Major thrusting events have been linked to sea level transgressions across the seaway (Kauffman, 1984; Villien and Kligfield, 1986; Elder et al., 1994; Pang and Nummendal, 1995; Liu et al., 2014).

The tectonically-driven bathymetry of the WIS, summarized in Figure 2, can be generalized as a western foredeep in Arizona, Utah, and western Colorado and Wyoming, a deep central axis along the modern Colorado Front Range, and a stable eastern “hinge zone” of slowly declining subsidence rates attached to the stable central craton of North America (Kauffman, 1984).

2.2 Sea Level and Lithology

Hancock and Kauffman (1979) and innumerable subsequent authors have shown that Western Interior third-order (1-2 myr) sea level cycles are generally synchronous with global eustatic cycles throughout the Cretaceous. If Cretaceous eustasy was largely driven by elevated seafloor spreading rates (e.g., Larson, 1991a, b), then changes in these rates would also have caused changes in the rate of subduction of the Farallon Plate beneath North America and thus changes in the rates of dynamic subsidence and tectonically-induced sea level changes in the WIS; indeed, times of eustatic rise are generally correlated with active plutonism/volcanism in the WIS (Kauffman, 1984). It is therefore difficult to say for sure whether eustasy or local tectonism was the primary control on sea level in the WIS, or whether it is even possible to meaningfully differentiate the two (e.g., Elder et al., 1994).

Tectonoeustatic sea level cycles were the main driver of sedimentation in the Western Interior, expressed as a regionally-correlative fining-upward sequence of clastics and increasingly calcareous facies during transgressive and highstand systems tracks, and the same facies sequence in reverse during regression (Kaufmann, 1977, 1984; Eicher, 1977). Transgressive sequences are more commonly interrupted with unconformities than regressions, which are generally more complete (Kauffman, 1969, 1977, 1984). Transgressive and highstand facies in the central axis and eastern portion of the basin are characterized by hemipelagic carbonates, with gradually decreasing carbonate content toward the foredeep basin to the west, which was characterized by a thick accumulation of medium- to fine-grained clastic sediments (Figure 2) (McGookey et al., 1972; Kauffman, 1984; Leckie et al., 1997; Molenaar et al., 2002).

2.3 Climate and Circulation

Regional, climate-induced sedimentary signals are superimposed on the tectonoeustatic sea level cycles as 4^{th}-5^{th} order cycles on Milankovitch time scales (e.g., Elder et al., 1994; Meyers et al., 2001, 2012; Locklair and Sageman, 2008; Sagemen et al., 2014; Ma et al., 2017). Cyclic changes in sedimentation on 1-10 m scales are very common in the WIS, and are commonly expressed as couplets

of, for example, limestone and shale (Kauffman, 1984). These couplets are primarily driven by changes in precipitation, evaporation, and climate induced water mass changes (e.g., Elderbak et al., 2014).

The precise mechanism(s) translating variations in precipitation and/or water mass to changes in terrigenous and/or pelagic sedimentation are still debated. The oldest and simplest hypothesis is that of Gilbert (1895), who proposed wet-dry cycles, where the wet period increased terrigenous flux, which diluted the pelagic carbonate sedimentation and resulted in the deposition of marl and mudrock, and dry periods with decreased terrigenous flux resulted in the deposition of limestones; in both cases, terrigenous flux is what changes while pelagic carbonate sedimentation remains the same (Pratt, 1984; Barron et al., 1985; Pratt et al., 1993). Other mechanisms are more complex and involve changes in circulation and carbonate productivity in the seaway (Eicher and Diner, 1989; Slingerland et al., 1996; Elderbak and Leckie, 2016).

Macro and microfossil paleobiogeography from the WIS and adjacent open ocean sites suggest two water masses entered the sea during late transgression (Figure 3): a warm, normal marine Tethyan water mass from the south and a cool, brackish Boreal water mass from the north. Quasi-estuarine circulation, driven by density differences between these watermasses and freshwater input on the margins of the seaway, caused these waters to form a counterclockwise gyre, with warm Tethyan waters to the east and cool Boreal waters to the west (Kent, 1968; Eicher and Worstell, 1970; Frush and Eicher, 1975; Kauffman, 1984; Pratt and Threlkeld, 1984; Eicher and Diner, 1985; Hay et al., 1993; Slingerland et al., 1996; Leckie et al., 1998; Elderbak et al., 2014; Da Gama et al., 2014; Lockshin et al., 2017). These two water masses likely mixed, through a process called caballing, to form a third, denser watermass that would have sunk and flowed out of the sea as a bottom current (Fisher, 1991; Hay et al., 1993; Elderbak and Leckie, 2016). Slingerland et al. (1996) proposed a modification of this caballing model where surface runoff from both margins of the sea, deflected to the right by the Coriolis force, created the engine to drive a counterclockwise gyre (Kump and Slingerland, 1999; Floegel et al., 2005;

253 Elderbak and Leckie, 2016). Increased freshwater flux would have strengthened the gyre, starving the
254 basin center of terrigenous sediments and allowing for the deposition of pelagic carbonates, essentially
255 the opposite of Gilbert's original dilution model. Nutrients were likely input into the system during
256 highstands with the incursion of oxygen-poor, nutrient-rich sub-thermocline waters in the Gulf of
257 Mexico (Lowery et al., 2017b). Additional nutrients were sourced from terrigenous influx and upwelling
258 along bathymetric highs (Leckie, 1998; Corbett and Watkins, 2013; Elderbak et al., 2014; Lowery et al.,
259 2014).

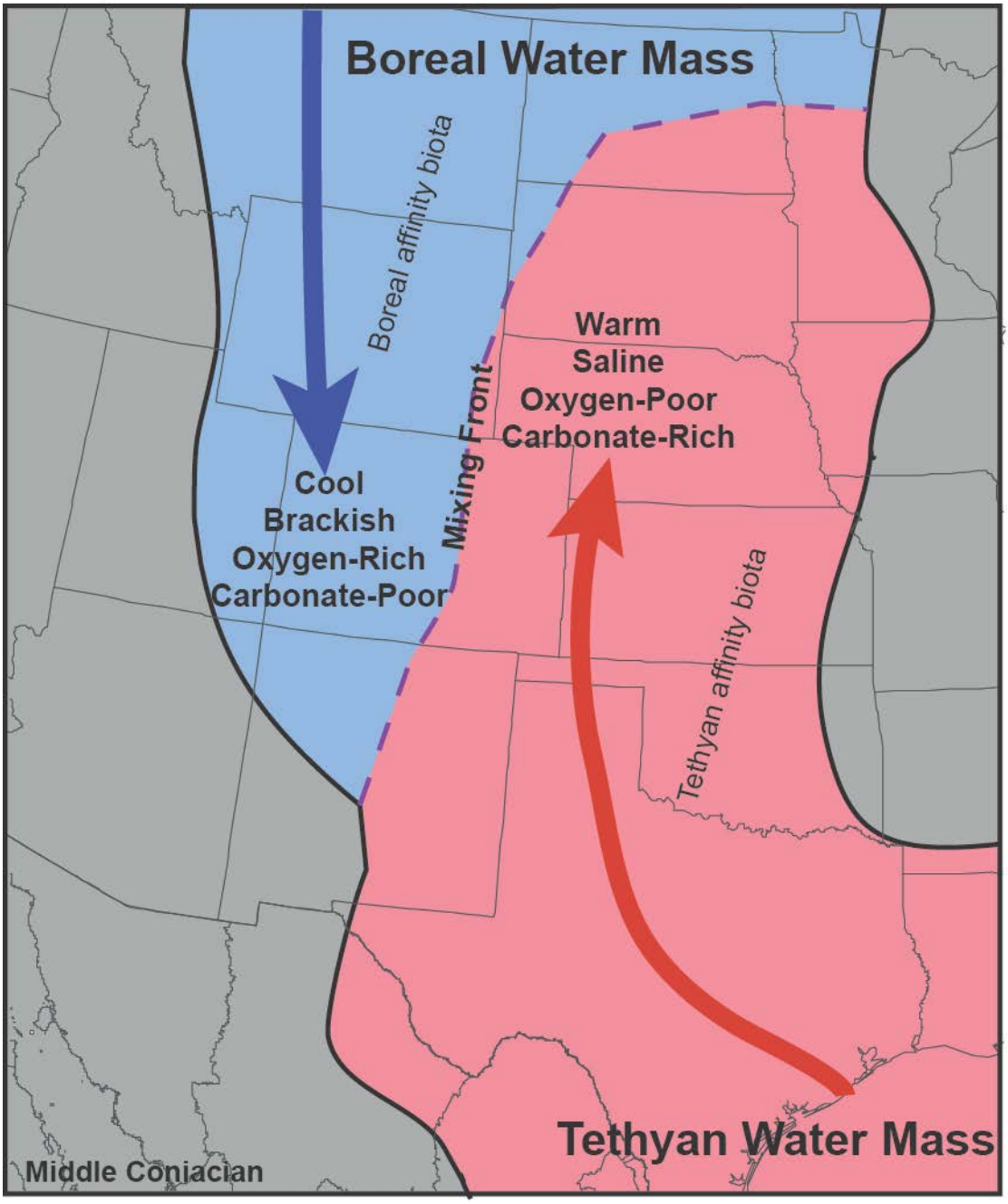


Figure 3. Summary of water mass and circulation in the Western Interior Sea, showing southern-sourced Tethyan water and northern-sourced Boreal water, and the approximate position of the boundary between the two along which mixing occurred. Based on Slingerland et al. (1996), Longman (1998), and Elderbak and Leckie (2016).

2.4 Two Major Sea Level Cycles

2.4.1 Greenhorn Cycle

The maximum flooding during Cenomanian-Turonian Greenhorn Cycle represented the highest sea levels in the history of the WIS (e.g., Kauffman, 1984). This cycle takes its name from the Greenhorn Formation, which deposited limestones and marls across much of the central and eastern Western Interior Sea (Figure 2). The Greenhorn is split into three members in the deep central axis of the seaway: the Lincoln Limestone, which is comprised of skeletal limestones deposited above storm wave base (Sageman, 1985), the deeper, anoxic Hartland Shale, and the comparatively-well oxygenated Bridge Creek Limestone, which represents late transgression and maximum flooding (Figure 4). Individual rhythmically-bedded limestone beds in the late transgression/highstand Bridge Creek Member can be traced over 1000 km (Hattin, 1971; Elder et al., 1994), and are expressed as marly or concretionary beds on the muddy western margin of the seaway in Utah and Arizona in the Mancos and Tropic Shales (e.g., Elder et al., 1994; Leckie et al., 1997; West et al., 1998).

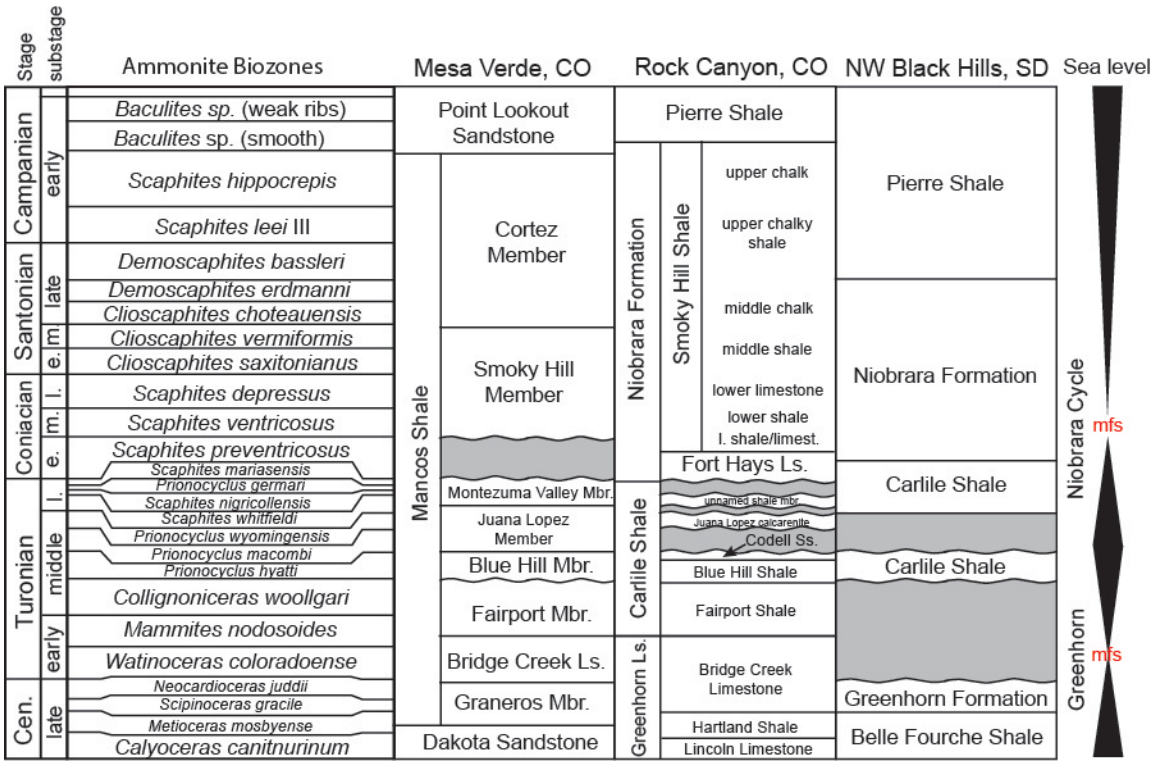


Figure 4. Summary of ammonite biozones, representative stratigraphic sections different regions of the study area, and broad sea level trends. Ammonite biozonation displayed is after Leckie et al. (1997) and

Merewether et al. (2011). Stratigraphic sections for Mesa Verde, Colorado in the western part of the seaway, Rock Canyon, Colorado in the deep central axis of the seaway (both after Leckie et al., 1997), and the northwestern Black Hills of south western North Dakota (after Merewether et al., 2011) show lithostratigraphy, including unconformities (squiggly lines and gray shading). Sea level trends are the general broadly accepted trends for the WIS; for example, see Kauffman (1984) or Caldwell and Kauffman (1993).

Rising sea level during the late Cenomanian gradually overcame a sill at the southern end of the seaway in Texas (e.g., Arthur and Sageman, 2005; Lowery et al., 2014) and brought an influx of normal-marine subtropical water into what had been a restricted, brackish seaway, causing a diversification of warm water mollusks, foraminifera, and calcareous nannoplankton. This transgression coincided with the onset of OAE2 and is also associated with an increase in bottom water oxygen in the central part of the seaway. At the Cenomanian-Turonian Global Stratotype Section in Colorado, the onset of OAE2 occurs at the transition from the anoxic, organic-rich Hartland Shale to the overlying organic-poor Bridge Creek Limestone, which records oxic conditions with a relatively abundant, diverse assemblage of benthic fossils and macrobenthic trace makers (e.g., Eicher and Diner, 1985; Pratt et al., 1985; Sageman, 1989; Arthur and Sageman, 1994, 2005; Leckie et al., 1998; Svarda, 1998a; Elderbak and Leckie, 2016). As sea level continued to rise toward the early Turonian highstand, sub-mixed layer, oxygen-depleted water that characterized the open Gulf of Mexico at this time (Lowery et al., 2017b) was carried into the seaway, resulting in dysoxia toward the end of OAE2 (e.g., Eicher and Diner, 1985; Arthur and Sageman, 2005).

The global anomaly in the carbon cycle during OAE2 was caused by the enhanced production of marine organic matter (Arthur et al., 1987; Schlanger et al., 1987; Jenkyns, 2010). This enhanced productivity, in turn, was driven by an increased flux of nutrients into the oceans due to high continental weathering rates (e.g., Pogge von Strandmann et al., 2013) caused by global warming related to the formation of the Caribbean Large Igneous Province (Bralower et al., 1997; Leckie et al., 2002; Snow et al., 2005; Barclay et al., 2010; Monteiro et al., 2012; van Bentum et al., 2012). These increased

weathering rates did not lead to eutrophication in the WIS, even though they were definitely expressed there. The formation of limestone-shale couplets in the Bridge Creek were deposited on obliquity (~41 kyr) timescales (Sageman et al., 1998, 2006; Meyers et al., 2001, 2012). These cycles were generated by dilution of pelagic carbonate deposition with terrigenous siliciclastics driven by orbitally-paced changes in continental runoff (Pratt, 1984; Barron et al., 1985; Watkins, 1989; Floegel et al., 2005; Elderbak and Leckie, 2016), although carbonate productivity also tended to be higher in the limestone intervals (e.g., Eicher and Diner, 1989; Elderbak et al., 2014; Elderbak and Leckie, 2016). While OAE2 was not associated with significant anoxia or organic matter deposition in the WIS, there was a significant turnover of marine plankton in the seaway (e.g., Leckie, 1985; Elder, 1991; Leckie et al., 1998; West et al., 1998) similar to that observed across the world (Leckie et al., 2002).

2.4.2 Niobrara Cycle

Following the middle Turonian regression of the Greenhorn Sea, a late Turonian-Coniacian transgression deposited hemipelagic chalks and marls across the Western Interior Basin from the Tethyan margin of Texas through Boreal Canada (McNeil and Caldwell, 1981; Kauffman and Caldwell, 1993; Longman, 1998; Schröder-Adams et al., 2014). Carbonate-rich sediments in the central and eastern part of the sea comprise the Niobrara Formation (Figures 2 and 4) (Hattin, 1975; Kauffman, 1977, 1984; Laferriere and Hattin, 1989). Niobrara-age marine sediments cover a smaller geographic area than the Greenhorn, indicating that the seaway was smaller and sea level lower than that previous cycle.

The record of the Niobrara Cycle is asymmetrical from Colorado to Kansas due to a large unconformity at the base of the Niobrara Formation that becomes wider (temporally) to the east. In many areas east of the Front Range the early transgressive phase of the cycle is preserved only as a very thin transgressive lag deposit (Juana Lopez calcarenite member of the Carlile Shale) or as reworked Codell Sandstone (which represents the lowstand of the Greenhorn cycle) in the basal Fort Hays

Limestone (Figure 4) (Hattin, 1975; Hattin and Cobban, 1977; Kauffman, 1977). In western Colorado and southern Wyoming, the Montezuma Valley Member of the Mancos Shale (Leckie et al., 1997) and Sage Breaks Shale (Fisher et al., 1985), respectively, occur between the Juana Lopez and Fort Hays Limestone, but these units are relatively thin (Figure 4). The Fort Hays Limestone Member represents the late transgression of the Niobrara Sea, with maximum flooding occurring in the lower portion of the overlying Smoky Hill Member (Kauffman, 1984; Lowery et al., 2017a); three chalky units of the Smoky Hill represent three fourth-order "transgressive pulses" (Hattin and Cobban, 1977; Kauffman et al., 1977; Molenaar, 1983; Dean and Arthur, 1998; Locklair and Sageman, 2008).

The Niobrara exhibits a variable lithology across its broad extent, but generally has the highest carbonate content to the east and south, particularly in Kansas, and decreasing carbonate with increasing proximity to the western margin of the seaway in western Colorado and Utah, where the Niobrara correlates to the marly Smoky Hill member of the massive Mancos Shale (Figure 3; Leckie et al., 1997). In central Colorado and Kansas it is divided into two formal units: the Fort Hays Limestone Member and the Smoky Hill Chalk Member (Scott and Cobban, 1964; Hattin, 1982; Dean and Arthur, 1998; Locklair and Sageman, 2008; Lowery et al., 2017a). In central Colorado, the Fort Hays is comprised of thick beds of limestone with very thin interbedded seams of black shale; to the south and west, marly interbeds may be of significant thickness (e.g., Scott et al., 1986; Sikora et al., 2004).

The Coniacian-Santonian interval records the last major, widespread deposition of black shales of the Mesozoic, sometimes referred to as OAE3 (Arthur and Schlanger, 1979). Organic-rich blacks shales of this age are well documented from the South Atlantic, Caribbean Sea, and surrounding epicontinental seas, with well-known localities summarized by Wagreich (2012), including the Western Interior US (e.g., Dean and Arthur, 1998; Locklair et al., 2011). During this same period, the eastern Tethys is characterized by the deposition of oceanic red beds, the result of generally oxic conditions associated with paleoceanographic changes brought about by the growing connection between the North and

South Atlantic ocean basins (Arthur and Natland, 1979; Wang et al., 2005, 2011; Trabucho-Alexandre et al., 2011).

Unlike older OAEs, there is no definable "event" with OAE3, just a general interval of enhanced black shale deposition. Although some of these black shales span the entire interval (and some, like Demerara Rise, are continuous from the Cenomanian-Turonian OAE2; e.g. Erbacher et al., 2004) others span only a portion of the event, and are often diachronous (Wagreich, 2012). Additionally, the positive carbon isotope excursion associated with OAE3 is more muted than that of previous OAEs, ~0.5‰ for OAE3 vs. ~2.0‰ for OAE2 (e.g., Joo and Sageman, 2014). For these reasons, it probably should not be termed an OAE (Wagreich 2009, 2012; Lowery et al., 2017a). However, it does represent a significant period of black shale deposition in coastal upwelling zones like Demerara and semi-restricted basins like Western Interior, and is perhaps useful a model of a non-OAE period of widespread anoxia.

3. MATERIALS AND METHODS

Benthic foraminifer abundance data is summarized from 32 localities (Figure 1) across the southern portion of the Western Interior Basin, ranging from Montana to New Mexico and Iowa to Utah. These represent a collection of published records and new data published here for the first time (including several unpublished graduate theses). Localities were only included in the study if they have 1) quantitative foraminiferal abundance data, and 2) well-defined molluscan biostratigraphic zonation. Biostratigraphic correlations are based on the most recent compilation (Merewether et al., 2011) of the well-established molluscan zones of Scott and Cobban (1964) (Figure 4). Benthic abundance is given as %benthics, which represents the percentage of benthic foraminifera out of the entire foraminifer population (i.e., planktics and benthics). Although an absolute measure of benthic abundance (e.g., benthics per gram of sediment) would have been preferable, such data was not available; nevertheless, we are confident that %benthics faithfully track changes in seafloor oxygenation in the WIS during this

time period (see section 3.1, below). All samples within a biozone at each site were averaged to a single value, giving our maps resolution on the order of 100 kyr (Appendix 1).

The Western Interior has a richness of paleontological data that few regions can replicate, and a relatively high density of localities that allow us to undertake this paleobiogeographic study. However, "good" geographic coverage for the Cretaceous can still be fairly sparse, and so maps are contoured by hand and contours should be considered subjective interpretations, particularly in areas without many data points. In intervals with very poor data coverage (near sea level lowstands), several biozones with few data points are combined into single maps. Maps presented here do not extend to Texas because well-constrained data there are only available for the late Cenomanian-early Turonian. However, published data from Texas for that interval (Frush and Eicher, 1975; Denne et al., 2014; Lowery et al., 2014) are used to inform contours in the southern part of the study area for those time intervals.

3.1 Benthic Foraminifera as Seafloor Oxygen Proxy

The abundance of benthic foraminifera in marine rocks is controlled by a variety of factors, including food supply, dissolved oxygen, salinity, pH, turbidity, and sea level (e.g., Jorissen et al., 1995, 2007; Leckie and Olson, 2003). Benthic abundance can be used as a proxy for any single one of these factors if the others can be independently controlled for. In the Cretaceous Western Interior, a number of workers have shown that the primary control on benthic abundance is dissolved oxygen (e.g., Eicher and Worstell, 1970; Eicher and Diner, 1985; Leckie et al., 1998; West et al., 1998; Elderbak et al., 2014; Elderbak and Leckie, 2016; Lowery et al., 2017a). To demonstrate that our benthic abundance data faithfully track changes in seafloor dissolved oxygen, we will evaluate the observed changes in the context of all of the factors that may affect benthic foraminifer abundance to rule them out. Often, other factors would be expected to drive %benthics in the opposite direction of what we observe, allowing us to reject those factors and attribute the observed changes to changes in oxygen. Additionally, other seafloor oxygen proxies (bioturbation index and the concentration of redox sensitive

trace metals) are available for some time intervals at some localities; these provide an independent test of our benthic foraminifer-based interpretations (Table 2). With two exceptions, these proxies agree with our interpretations. The two exceptions are enrichments of Mo which indicate sedimentary euxinia while low abundances benthic foraminifer abundances suggest seafloor dysoxia. Changes in redox state several mm below the seafloor are common in many modern environments, and so these two redox states in the same interval are not mutually exclusive.

Food supply is a major factor controlling benthic foraminiferal abundance, and is often linked to anoxia due to oxygen depletion in eutrophic waters (Jorissen et al., 1995; Gooday, 2003; Jorissen et al., 2007). Fortunately, it is also the easiest factor to control for: if organic matter is enriched in sediments it strongly suggests that food supply was not the limiting factor for benthic abundance (Lowery et al., 2017a). Organic matter is enriched across much of the study area, and in fact is generally highest in sediments with the lowest benthic abundance. Thus, organic matter cannot explain the observed trends in benthic foraminifera.

Some organic rich low oxygen environments are characterized by a low diversity, high abundance assemblage of foraminifera. A contemporaneous example of this can be found at Demerara Rise, where much of the mid-Cretaceous section is highly enriched in organic carbon, and some samples contain very high abundance populations of benthics comprised of one or a few species. To determine whether such assemblages occur in our samples, we plot simple diversity and Shannon diversity (which takes evenness into account) against benthic abundance for our WIS sites, and compare these with samples from Demerara Rise ODP Sites 1258-1261 (Friedrich et al., 2006, 2009) (Figure 5). These plots show distinct trends at Demerara and the WIS. In contrast to the low diversity Demerara Rise samples, the WIS is characterized by low abundance assemblages of varying diversity and high abundance assemblages of mostly high diversity. No sample containing >10% benthics in the WIS is comprised of a single species, and only five samples >10% contain less than five species. In contrast, most Demerara

Rise samples are comprised of less than 5 species, and many high abundance samples are monospecific. Therefore, we are confident that no dysoxic high-abundance assemblage occurs in the WIS.

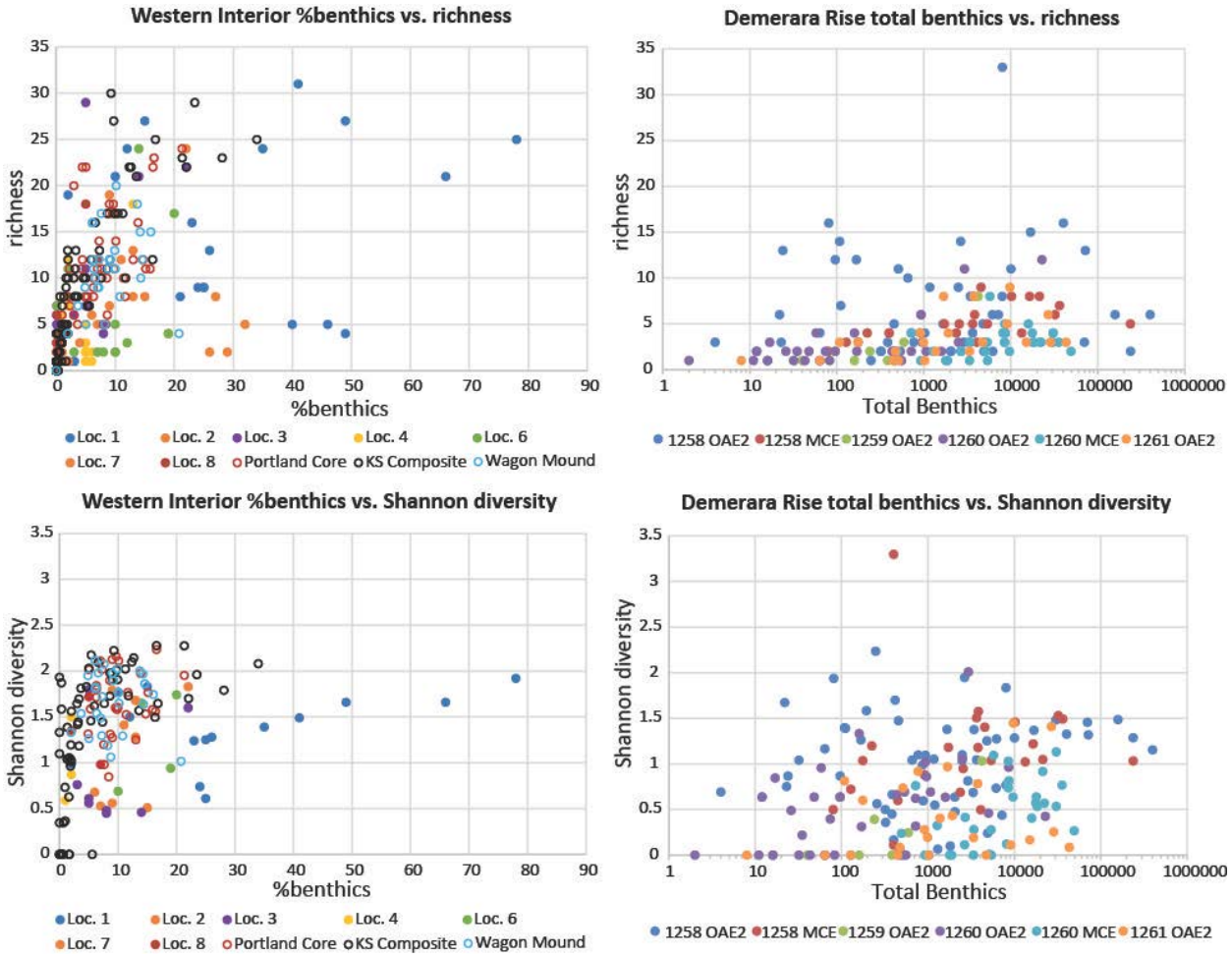


Figure 5. Cross plots of benthic foraminiferal abundance with benthic richness (top) and Shannon diversity (bottom) in the Western Interior (left) and Demerara Rise (right). Western Interior data primarily comes from the Greenhorn cycle sites of Eicher and Worstell (1970; their Localities 1-8, with the exception of Loc. 5, which did not include benthic foraminifera diversity data) and the Niobrara interval of the Portland Core (Lowery et al., 2017a). Demerara data from the Mid-Cenomanian Event (MCE) at ODP Sites 1259 and 1260 (Friedrich et al., 2009) and OAE2 at ODP Sites 1258, 1259, 1260, and 1261 (Friedrich et al., 2006). Note that while WIS data are plotted against %benthics, lack of planktic foraminiferal counts from the Demerara sites meant that those data had to be plotted against benthics per gram on a log scale.

Changes in salinity may also effect benthic foraminiferal abundance. Benthics are generally tolerant of a wider range of salinities than planktic foraminifera, and as such tend to dominate sediments in brackish waters like estuaries or lagoons, as well as hypersaline waters (e.g., Poag, 1981;

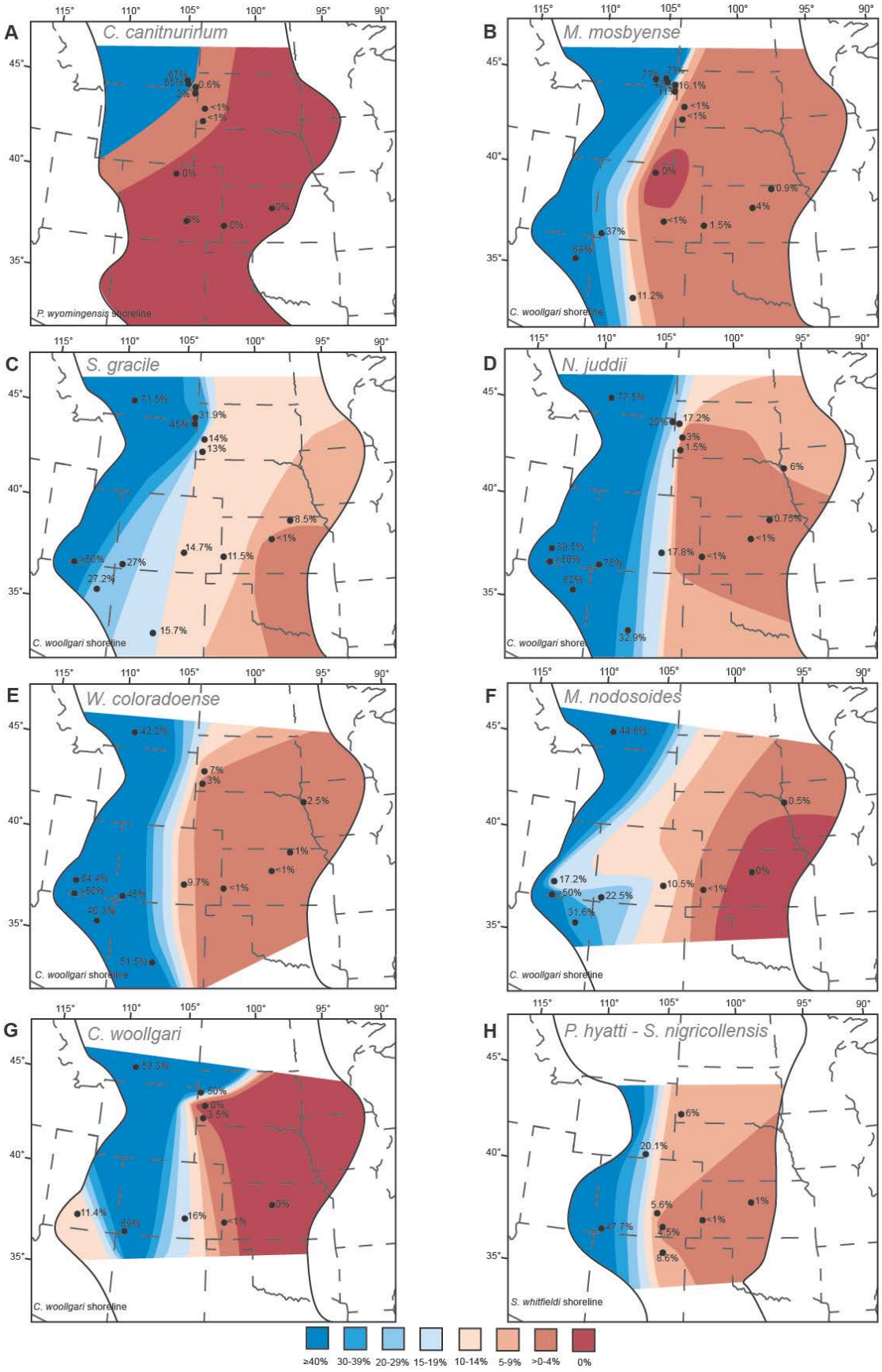
444 Gooday, 2003; Leckie and Olson, 2003). This has also been well-documented on the western margin of
445 the WIS (e.g., Tibert et al., 2003; Tibert and Leckie, 2004, 2013). Changes in salinity, therefore, would be
446 expected to result in increased %benthics (e.g., Caldwell, et al., 1993; Nielsen et al., 2008; Schröder-
447 Adams et al., 2014; Da Gama et al., 2014), and therefore could not be mistaken for anoxia in our data.
448 Generally, the most restricted time intervals (and therefore the most brackish/favorable for benthics)
449 contain the fewest benthics, trends that cannot be explained by salinity changes.
450 Changes in pH are also known to effect benthic assemblages, but corrosive bottom waters are
451 not barren, they are merely dominated by agglutinated benthic foraminifera (Gooday, 2003).
452 Additionally, the shallow waters of the WIS are well above the depth of the lysocline, and there is no
453 evidence in the seaway for acidification or post-depositional dissolution (e.g., an increase in planktic
454 fragmentation index), so changes in carbonate ion saturation are a very unlikely explanation for the
455 trends in the data. Post-depositional changes in pore water pH (especially in organic-rich sediments)
456 may be expected to impact preservation of calcareous fossils. Such diagenetic dissolution typically
457 results in an increase in foraminifer fragments (e.g., Berger et al., 1982). We do not observe foraminifer
458 fragments in the WIS, suggesting that carbonate dissolution and fragmentation is not a problem there.
459 We do, occasionally, observe completely barren samples which lack both planktic and benthic
460 foraminifera, sometimes with a few pyrtized foraminifera or steinkerns; such samples are excluded from
461 our data. Even if poor preservation was altering our assemblages, it would skew the data toward higher
462 %benthics because planktic foraminifera, which tend to be smaller and less robust than benthics, would
463 be preferentially fragmented. We observe the opposite trend in the organic-rich facies in which such
464 dissolution would be likely to occur, as %benthics tends to decrease in organic rich facies, indicating that
465 poor preservation is not a satisfactory explanation for the observed trends.
466 Sea level has a well-known relationship with benthic foraminifer abundance (e.g., Van de Zwaan
467 et al., 1990; Leckie and Olson, 2003; Van Hinsbergen et al., 2005), with declining %benthics with

increasing water depth/distance from shore. However, in moderate water depths like those found in the WIS (<200 m; Sageman and Arthur, 2004), %benthics typically range from 20-80% depending on local factors like salinity, food supply, and, critically, oxygen (e.g., Culver, 1988; Leckie and Olson, 2003; Van Hinsbergen et al., 2005). The wide range (20-80%) of typical abundances likely reflects variations in those other factors. Benthic abundances below 20% at shelf water depths would imply stress of the seafloor. Because we know the WIS was generally brackish (which would lead to higher than normal %benthics) and enriched in organic matter (which would also lead to higher than normal %benthics), the lower than average benthic abundances we observe must be due to oxygen stress. Additionally, we observe an increase in %benthics across the seaway during transgressions and a decline in %benthics during regression and lowstand, which is the opposite of what we would expect to observe if the changes were driven by sea level and not oxygen.

Because we can rule out these other factors, plus the agreement of other proxies for seafloor oxygen with our foraminifer-based interpretations (Table 2), we are confident that changes in dissolved oxygen are the primary control on benthic foraminifer abundance in the WIS during the study interval. This is not necessarily the case in other localities and in other time periods and the reader should conduct a similar evaluation of all the parameters effecting benthic foraminifer abundance before making similar interpretations of dissolved oxygen at other localities.

4. RESULTS

Benthic foraminifer abundance data are averaged by ammonite biozone and presented geographically in Figures 6 (Greenhorn Cycle) and 7 (Niobrara Cycle). Trends for each cycle are summarized below.


A
C. canitnurinum
P. wyomingensis shoreline
B
M. mosbyense
C. woollgari shoreline
C
S. gracile
C. woollgari shoreline
D
N. juddii
C. woollgari shoreline
E
W. coloradoense
C. woollgari shoreline
F
M. nodosoides
C. woollgari shoreline
G
C. woollgari
C. woollgari shoreline
H
P. hyatti - S. nigricollensis
S. whitfieldi shoreline
≥40%
30-39%
20-29%
15-19%
10-14%
5-9%
>0-4%
0%

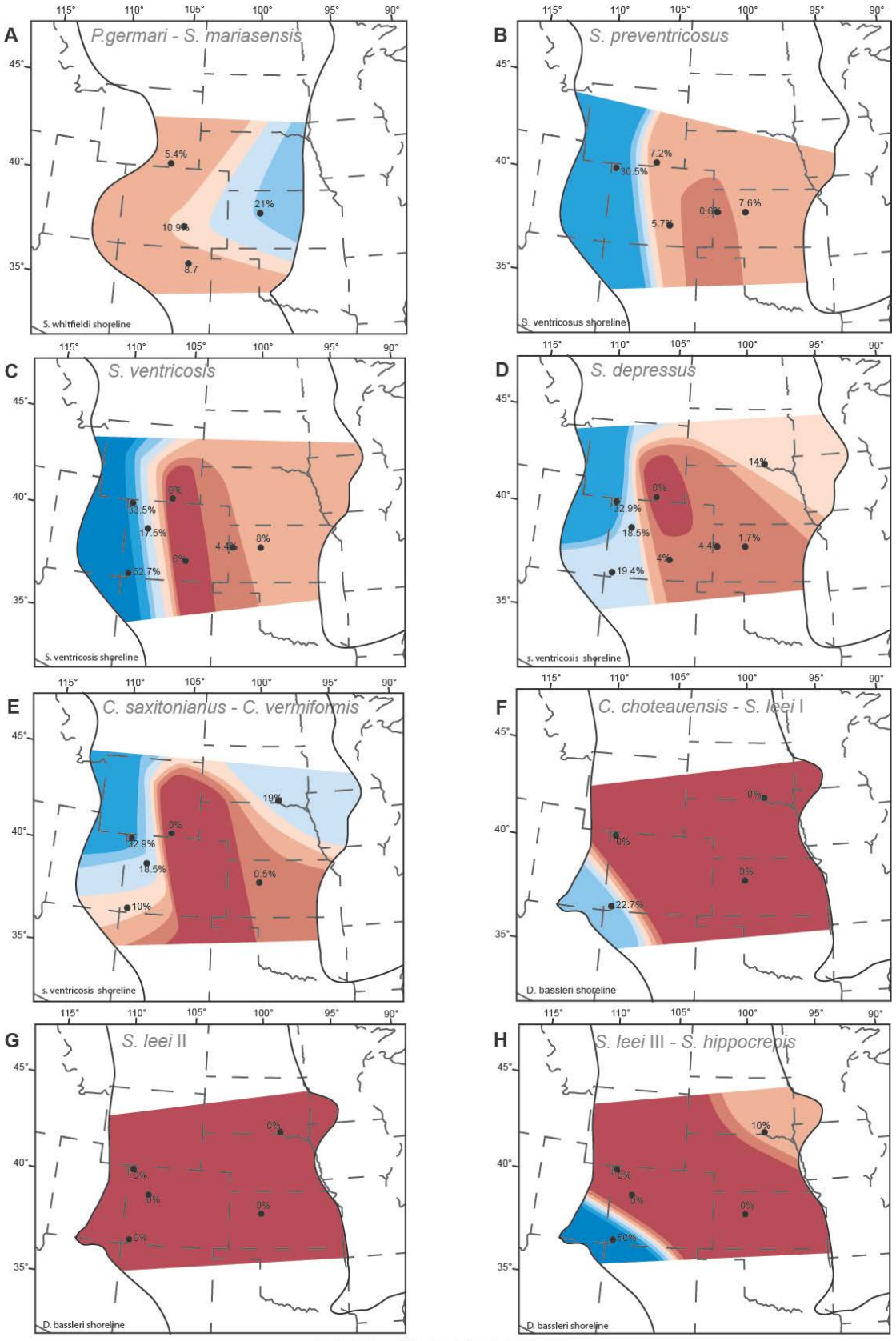
489

Figure 6. Maps summarizing bottom water oxygenation trends throughout the Greenhorn Cycle. See text for discussion; see Figure 4 for explanation of ammonite genus abbreviations. Shorelines based on paleogeographic maps by Blakey (2016).

4.1 Greenhorn Cycle – Late Cenomanian to Middle Turonian

The Greenhorn cycle begins with benthic foraminifera restricted to the northwestern portion of the study area in the early late Cenomanian *Calyoceras canitnurinum* Zone (Figure 6A). The lack of benthic foraminifera in the southern seaway indicates anoxic bottom waters. This interpretation is confirmed by the lack of bioturbation in the USGS Portland #1 Core in Fremont, CO and the Amoco Rebecca Bounds #1 Core in Kansas (Svarda, 1998a) (Table 2). Benthic abundance increases across the seaway in the *Metioceras mosbyense* Zone (Figure 6B) and peaks in the late Cenomanian *Scipinoceras gracile* Zone (Figure 6C). The *S. gracile* Zone corresponds with the onset of OAE2, and is associated with a number of proxies for increasing oxygen, including very low Molybdenum concentrations (Mo is enriched in anoxic environments with sulfate reduction, termed “euxinic”; Meyers et al., 2001, 2005) and an increase in bioturbation in both the Portland and Bounds Core (Svarda, 1998a) (Table 2). The abundance of benthics, which is higher in eastern Colorado than Kansas, is echoed in the bioturbation index, which is also higher in eastern Colorado than in Kansas (Svarda, 1998a) (Table 2). Following the peak during the *S. gracile* Zone, benthic abundance in the eastern seaway slowly declines through the latest Cenomanian and early Turonian to the middle Turonian *Colignoceras woollgari* Zone, where anoxia is present throughout the eastern seaway. Mo concentrations in the Portland Core are elevated starting in the late early Turonian *Mammites nodosoides* Zone (Meyers et al., 2001, 2005), although %benthics are still relatively high at this point (Figure 6F), suggesting euxinic conditions in the sediments but not at the sediment water interface at this point in time (Table 2). Svarda (1998a) noted decreasing bioturbation throughout the Bridge Creek limestone (i.e., *S. gracile* to *M. nodosoides* Zones) following a peak at the base in both the Portland and Bounds cores, again mirroring %benthic trends (Table 2).

Throughout the Greenhorn Cycle, benthic abundances are significantly higher on the western margin of the seaway compared with the central axis or the eastern margin, indicating well-oxygenated conditions there throughout this interval. The data are mostly widely distributed, but the close cluster of points in the Montana-Wyoming-South Dakota region indicate that the oceanographic front that was set up across the seaway was likely very steep, as %benthic values change significantly over tens of kilometers (Fisher et al., 1994; Fisher and Arthur, 2002).


A
P.germari - S. mariasensis
5.4%
21%
10.9%
8.7
S. whitfieldi shoreline
B
S. preventricosus
7.2%
30.5%
7.6%
0.6%
5.7%
S. ventricosus shoreline
C
S. ventricosis
0%
33.5%
17.5%
4.4%
8%
6%
52.7%
S. ventricosis shoreline
D
S. depressus
14%
0%
32.9%
18.5%
4.4%
1.7%
4%
19.4%
s. ventricosis shoreline
E
C. saxitonianus - C. vermiformis
19%
0%
32.9%
18.5%
0.5%
10%
s. ventricosis shoreline
F
C. choteauensis - S. leei I
0%
0%
0%
22.7%
D. bassleri shoreline
G
S. leei II
0%
0%
0%
0%
0%
D. bassleri shoreline
H
S. leei III - S. hippocrepis
10%
0%
0%
0%
50%
D. bassleri shoreline
≥40%
30-39%
20-29%
15-19%
10-14%
5-9%
>0-4%
0%

522

Figure 7. Maps summarizing bottom water oxygenation trends throughout the Niobrara Cycle. See text for discussion; see Figure 4 for explanation of ammonite genus abbreviations. Shorelines based on paleogeographic maps by Blakey (2016).

4.2 Niobrara Cycle – Late Turonian to Early Campanian

The Niobrara Cycle begins (Figure 7A) with generally higher benthic foraminifer abundance than in the preceding middle Turonian *Prionocyclus hyatti* through early late Turonian *Scaphites nigricollensis* (Figure 6H) map. For the only time in the study interval, there are higher benthic abundances on the eastern margin than on the western margin, likely due to a lack of data from the western margin of the seaway for this zone. This quickly changes through the early Coniacian transgression of the Niobrara Cycle in the Fort Hays Limestone equivalent *Scaphites preventricosus* Zone, with almost no benthic foraminifera in the central seaway (confirmed by a lack of bioturbation in the Bounds Core; Svarda, 1998b; Table 2) and generally higher %benthics toward the western margin (Figure 7B). The near lack of benthics in the *S. preventricosus* Zone becomes a complete absence in the middle Coniacian *Scaphites ventricosus* zone, and spreads north from eastern Colorado into southeastern Wyoming (Figure 7C). As opposed to the Greenhorn Cycle, when values declined eastward, here values are lowest in the deep central axis of the seaway, and increase further east (although they still remain much lower than the well-oxygenated western margin).

Seafloor conditions recovered slightly in the late Coniacian *Scaphites depressus* Zone (Figure 7D), as the anoxic zone contracted to roughly the area of the Denver Basin (an interpretation influenced by the trace metal data of Locklair et al., 2011; Table 2). This short-lived recovery gave way to a greater expansion of anoxia beginning in the early Santonian *Clioscaphites saxitonianus* Zone and continuing through the *Scaphites leei* II Zone in the early Campanian (Figure 7E-G), when no benthic foraminifera are present anywhere in the study interval, indicating widespread, entrenched anoxia (Lowery et al., 2017a). This long decline through the Niobrara Cycle is supported by trends in bioturbation and trace

548 metals (Table 2). Bioturbation in both the Bounds Core and Portland Core declines throughout both
549 cores from a high in the Fort Hays Limestone (Svarda, 1998b). At both localities, limestone/chalk
550 intervals are more bioturbated than marlstones (Svarda, 1998b). Trace metal proxy data from the
551 Encana Aristocrat Angus core in the Denver Basin (Table 2) indicates enrichment of Manganese in the *S.*
552 *preventricosus* Zone which declines toward a transition in the *S. ventricosus* Zone. Above this level, the
553 core is enriched in Vanadium + Chromium, which slightly precedes a sharp increase in Mo, which
554 indicate anoxia and euxinia, respectively (Locklair et al., 2011). Similar trends exist in the Portland Core,
555 which also records a decline in Mn in the *S. preventricosus* Zone and a sudden enrichment in Mo in the
556 *S. ventricosus* Zone (Tessin et al., 2015). Trace metal data from the Portland Core indicates that the
557 organic matter enrichment there was due to the development of anoxia and subsequent Fe recycling
558 from euxinic sediments, which provided a source of nutrients for sustained productivity (Tessin et al.,
559 2015, 2016). At the end of the Niobrara Cycle in the early Campanian *Scaphites leei* III – *Scaphites*
560 *hippocrepis* Zones, benthic foraminifera reappear on both margins of the seaway but otherwise remain
561 absent in the center of the seaway (Figure 7H). This is corroborated by redox sensitive metals from two
562 cores in the Denver Basin: the Aristocrat Angus core and the Berthoud State core, which indicate anoxia
563 (Table 2).

564 **5. DISCUSSION**

565 Benthic foraminifer abundance, and by proxy bottom water oxygen content, was controlled
566 primarily by watermass in the Western Interior Sea. Benthic foraminifera tend to be more abundant to
567 the north and along the western side of the seaway, corresponding to the areal extent of Boreal waters
568 which were cool, brackish, and oxygen rich (Longman, 1998). Tethyan waters were warm, saline, and
569 generally oxygen poor, and were present in the southern and eastern sides of the seaway (Longman,
570 1998; Elderbak et al., 2014), which tended to contain much fewer benthic foraminifera. Trends in the
571 relative influence of these waters can be identified as relative sea level changed during both cycles. The

572 Greenhorn Cycle is characterized by a strong and persistent paleoceanographic front that developed in
573 the central seaway, particularly during periods of higher sea level (Fig. 6B-E). The Niobrara Cycle is also
574 characterized by an oceanographic front in the same region during the late Turonian-middle Coniacian
575 transgression (Fig. 7B-C), but during the highstand and subsequent regression, this front is replaced (on
576 the seafloor at least) by a persistent and expanding region of anoxic bottom waters indicating the
577 stratification and stagnation of the central sea, which then spread as sea level fell (Fig. 7C-H).
578 Sea level exerted a strong control on the influence and interaction of these watermasses,
579 evidenced by the clear relationship between sea level and the relative mixing of northern and southern
580 watermasses. The strength of this mixing must have been controlled by the volume of each water mass
581 that was able to enter the seaway, which would have been greater during periods of higher sea level. A
582 sill at the southern mouth of the WIS restricted the amount of Tethyan water that was able to enter the
583 seaway during periods of lower sea level (Sageman and Arthur, 2005; Lowery et al., 2014; Elderbak and
584 Leckie, 2016). During the Greenhorn transgression, the southern sill was overtopped at the time of the
585 upper Cenomanian *S. gracile* Ammonite Zone and Tethyan water rapidly overspread the southern and
586 eastern seaway. (Figure 6; Eicher and Diner, 1985; Leckie et al., 1998; Elderbak et al., 2014; Lowery et
587 al., 2014; Elderbak and Leckie, 2016).
588 This incursion of oxygen-poor Tethyan water is paradoxically associated with increasing benthic
589 oxygen values across the entire seaway. This is counter to both the known oxygen-poor nature of this
590 water mass and the general model of stratification developing in a deepening basin (e.g., Arthur and
591 Schlanger, 1979). Prior to the Tethyan incursion, widespread seafloor anoxia developed through the *C.*
592 *canitnurinum* and *M. mosbyense* Zones (Fig. 5A-B) due to the restricted nature of seaway and productive
593 surface waters. During the late transgression of the Greenhorn Sea in *S. gracile* through *W. coloradoense*
594 time, anoxia (at least on time scales represented by discrete outcrop and core samples) did not exist in
595 the Western Interior Sea (Fig. 6C-E). The well-oxygenated conditions of the *S. gracile* Zone eventually

gave way to dysoxic conditions in the central and eastern seaway with the approach of peak transgression and highstand during the early Turonian *M. nodosoides* Zone (Fig. 6F) and became more widespread as regression continued through the middle Turonian *C. woollgari* Zone (Fig. 6G).

During the Niobrara Cycle, benthic oxygen is also generally highest during the transgression, peaking in the uppermost Turonian *S. mariasensis* Zone in the Fort Hays Limestone Member of the Niobrara Formation (Fig. 7B). As sea level rise peaked, anoxia appeared in the deep central axis of the basin (Fig. 7C) and expanded during the subsequent regression (Fig. 7D-G, which is completely anoxic). This pattern, with anoxia first forming in the deepest part of the basin, is consistent with a model of increasing stratification and stagnation through late transgression and highstand. This interpretation agrees with geochemical observations indicating that anoxia was primarily driven by increases in the preservation potential of organic matter and subsequent iron recycling from euxinic sediments (Tessin et al., 2015, 2016). Benthic foraminifera only reappear at the end of the Niobrara Cycle (Fig. 7H) at nearshore localities, likely indicating the influence of physical mixing by wave and tidal action in shallow coastal waters. The Niobrara was significantly more anoxic than the Greenhorn Cycle; we interpret this as due to the fact that it did not experience as large a sea level rise and was therefore more restricted.

Overall, when sea level was high during the Greenhorn transgression, an oceanographic front formed in the seaway and benthic oxygen values, though partially controlled by water mass affinity, are generally higher (e.g., Fig. 6D). When sea level is low, the oceanographic front is less evident, the seaway became more restricted and/or stratified, and benthic oxygen values were generally lower. During the Niobrara Cycle, in which the seaway was more restricted and sea level never rose as high as the Greenhorn, an oceanographic front was never firmly established, and widespread anoxia developed during regression (e.g., Fig. 7G). What controlled these changes?

5.1 Mixing and Downwelling

Paleoceanographers generally agree that the interaction of northern and southern water masses in the Western Interior resulted in mixing and the downwelling of a third water mass, here referred to as Western Interior Intermediate Water (WIIW), although the exact mechanism has been debated (e.g., Hay et al., 1993; Fisher et al., 1994; Slingerland et al., 1996; Elderbak and Leckie, 2016). Downwelling surface water, which was physically mixed by wind and waves, must have been at least somewhat oxygenated. Intermediate water formation and downwelling, then, would have increased oxygen concentrations on the seafloor.

The mixing of watermasses that created this downwelling was ultimately controlled by the volume of northern and southern waters entering the seaway, as indicated by the strong oceanographic front that developed along the central axis of the seaway during periods of high sea level. These periods are characterized by relatively high bottom water oxygen and benthic foraminifer abundance (Figure 8). When sea level was lower, less water entered the seaway, mixing and downwelling was weaker, and, as oxygen export to the seafloor fell below a threshold, anoxia formed in the central basin (Figure 8). During both the Greenhorn and Niobrara cycles, periods of highstand and falling sea level are associated with greater restriction and widespread anoxia in the basin, and periods of late transgression are associated with relatively oxic conditions (Figure 8).

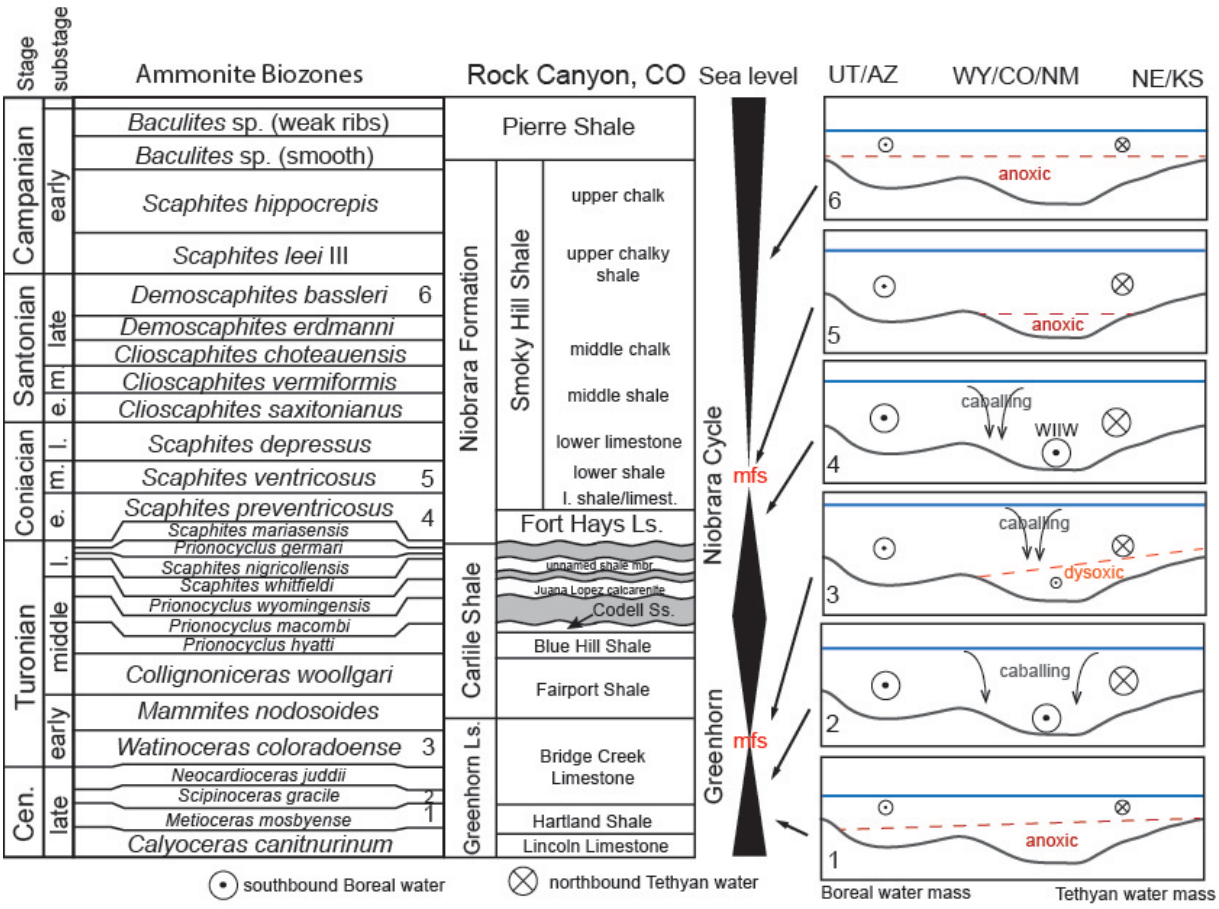


Figure 8. Conceptual model of the relationship between sea level and oxygen in the Western Interior Sea along an east-west transect. When sea level is high, mixing water masses along an oceanographic front in the central axis of the seaway results in a downwelling of a third water mass that exports oxygen to the seafloor. As sea level falls the amount of oxygen exported to the seafloor declines, and eventually falls below benthic oxygen demand, anoxia develops on the seafloor. Numbers in the ammonite biozones correspond to respective boxes summarizing conditions during those time intervals.

5.2 Models for black shale development and anoxia

This model for the development of anoxia in epeiric seas is significantly different than the traditional model for equating transgression with deoxygenation on open shelf settings (e.g., Arthur and Schlanger, 1979; Arthur and Sageman, 2005). Arthur and Sageman (2005), who use the WIS as an example of black shale development in a restricted basin, note that sea level rise can cause brief oxygenation events during transgression in restricted basins; our interpretations provide a mechanism for this observation. Unlike stratified shelf environments, which are not typically aerated by bottom

currents, semi-restricted basins like the WIS can experience the mixing and downwelling of surface watermasses and overcome the stratification caused by rising sea level.

Building off of the model of Arthur and Sageman (2005), who suggested the rising sea level brought dysoxic OMZ water into the Western Interior Seaway, our data demonstrate that the eutrophication and anoxia of peak transgression and highstand were preceded by a mixing event that ventilated the stratified seaway during mid-late transgression (Figure 8). In a pattern repeated during both the Greenhorn and Niobrara cycles, we observe 1) anoxia during sea level lowstands and early transgression due to stratification and poor communication with the open ocean (e.g., Hartland Shale Mbr., Greenhorn Fm. – Figure 6A; upper Smoky Hill Mbr., Niobrara Fm. – Figure 7F-H), 2) a flushing of the seaway during mid-transgression driven by both downwelling oxygenated surface water and improved communication with the open ocean (e.g., lower Bridge Creek Mbr., Greenhorn Fm. – Figure 6C; Fort Hays Mbr., Niobrara Fm. – Figure 7A-B), and 3) dysoxia during peak transgression and highstand as eutrophication took hold due to the inflow of low-oxygen OMZ waters over the southern sill and marine productivity (e.g., Fairport Shale Mbr., Carlile Shale, – Figure 6F-G; lower Smoky Hill Mbr. – Figure 7C-E). This dysoxia, rather than long-lasting anoxia, was characterized by at least intermittent oxygenation events allowing a small benthic population to persist on the seafloor, even along the eastern margin of the sea. As highstand transitioned to regression, the seaway once again became cut off from the open ocean and restricted. WIIW development would have been weakened by declining relative sea level due to shoreline progradation during highstand, and nutrient recycling from the organic-enriched seafloor would have sustained primary productivity (Tessin et al., 2015). The resulting reduction in mixing and downwelling led to stratification, and anoxia developed and became entrenched.

5.3 Epieric Seaway vs. Continental Margin

674 The drivers of oxygen change are different in the WIS and other restricted epicontinental
675 seaways than at continental margin sites like Demerara Rise (Figure 9). Demerara Rise is a relatively
676 deep continental margin intersected by an expanded oxygen minimum zone (OMZ). Upwelling and high
677 productivity along this margin drove the development of this OMZ and resulted in black shale deposition
678 from the Cenomanian to Santonian (Kuypers et al., 2002; Erbacher et al., 2004, 2005; Friedrich et al.,
679 2006, 2009). This nutrient-rich environment favored the development of high abundance, low diversity
680 benthic assemblages (Figure 5). Epeiric seas like the WIS are significantly different from this continental
681 margin OMZ. Changes in dissolved oxygen in the WIS were driven by changes in sea level and the
682 movement of outside water masses into the seaway. Rather than upwelling driving increased
683 productivity, reduced mixing and downwelling allowed the development of stratification, resulting in an
684 increase in preservation (Figure 9). Rather than the low diversity, high abundance assemblages of
685 dysoxic productive margins like Demerara, the WIS contains variable diversity assemblages where
686 abundance is primarily related to oxygen availability (Figure 5).
687 Thus the WIS can be considered a model for the development for anoxia in epeiric seas in the
688 Cretaceous, and more broadly other shallow semi-restricted basins with estuarine or quasi-estuarine
689 circulation. The WIS is probably uniquely large for a shallow epicontinental sea, and certainly unique in
690 that it extends from the arctic to the subtropics. However, it is still a useful example of, and at least a
691 partial analog for, the processes that occur in shallow semi-restricted basins of all sizes. Although they
692 are significantly smaller, modern basins like the Baltic Sea or Chesapeake Bay are similar to the WIS in
693 that they characterized by the interaction of a warm, normal salinity watermass and a cool, brackish
694 water mass, with oxygenation change driven by stratification-induced eutrophication.
695 Importantly, the period of excess carbon burial that has come to be known as OAE2 was
696 primarily driven by enhanced marine productivity of the type typified at Demerara Rise (e.g., Jenkyns,
697 2010). The lack of anoxia and black shale deposition associated with OAE2 in the WIS can be attributed

to the different mechanisms driving oxygen concentration and preservation-driven organic matter enrichment there. This suggests that epeiric seas were less important to the development of OAEs than continental margin sites.

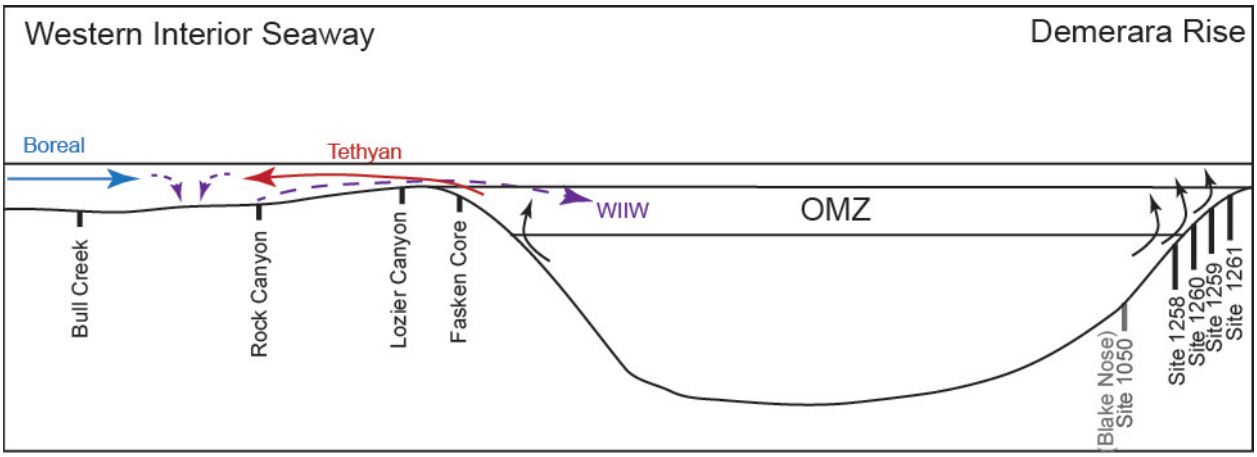


Figure 9. Schematic comparison of oceanography of the WIS with more typical open ocean sites, ODP Sites 1258-1261 (Demerara Rise) and Site 1050 (Blake Nose). The WIS is characterized by two water masses mixing and downwelling and the occasional encroachment of an OMZ during times of high sea level. The mid-depth continental margin sites of Demerara Rise are impinged by an OMZ and constantly sourced with nutrients due to upwelling, and are this highly productive. Blake Nose is a lower bathyal site well below the influence of the OMZ and did not experience anoxia during OAEs.

6. Conclusions

- Bottom water oxygenation in the Cretaceous Western Interior Sea was controlled by a combination of water mass source and mixing, sea level, and basin restriction. The northern and western parts of the seaway, flooded by cooler northern affinity water masses, tended to have higher oxygen concentrations than the eastern and southern portions of the seaway, which were flooded by warmer southern affinity waters. On the whole, all parts of the seaway were better oxygenated during periods of mid to late transgression, and more poorly oxygenated during peak transgression and highstand, and, dysoxic to anoxic during regression.
- These first-order trends in seafloor oxygenation were driven by the formation and downwelling of Western Interior Intermediate Water, which oxygenated the seafloor during times of

improved communication with the open ocean. This new water mass was formed by the mixing of northern and southern waters; mixing was strongest when sea level was high and larger volumes of water could enter the seaway (demonstrated by the sharp oceanographic front that formed in the center of the seaway). The oxygenating effect of this downwelling was strongest earlier in the transgression, before deeper low-oxygen OMZ waters were able to spill into the seaway at peak transgression, generating dysoxia. During subsequent regression, less water entered the seaway, mixing declined, downwelling weakened, and the seaway became restricted, stratified, and anoxic. Anoxia first formed in the deep central axis of the seaway and eventually spread through the entire basin. These patterns repeat across the Greenhorn and Niobrara cycles, which suggests they were controlled by the physical and oceanographic set up of the basin and not by ephemeral climate events.

- These patterns explain why the oxygenation in the WIS was antiphase with the global OAE2, and illustrate how epeiric seas like the WIS were a completely different oceanographic systems from typical continental OMZ and upwelling zones where deoxygenation is primarily the result of increased productivity. This provides a model for how deoxygenation may occur in shallow, estuarine-circulation driven semi-restricted basins of any size.

Acknowledgements

RML would like to acknowledge his former PhD advisor, Prof. Don L. Eicher, for all his pioneering work on Cenomanian-Turonian foraminifera of the U.S. Western Interior, and similarly to Prof. William Frerichs for his many contributions to the study of Niobrara-age foraminifera of the seaway. The senior authors would like to thank numerous colleagues for their contributions to the study of the Cretaceous Western Interior Sea, and for discussions over the years about foraminifera and seaway paleoceanography, especially Mike Arthur, Liz Balcells-Baldwin, Tim Bralower, Matt Corbett, Walt Dean,

Richard Diner, Jeff Eaton, Don Eicher, Will Elder, Cindy Fisher, Don Hattin, Bill Hay, Steve Hook, Erle Kauffman, Jim Kirkland, Lonnie Leithold, 'K' Molenaar, Lisa Pratt, Brad Sageman, Claudia Schröder-Adams, Rudy Slingerland, Neil Tibert, Laura Von Holdt, and David Watkins. We acknowledge the donors to the American Chemical Society-Petroleum Research Fund for primary research funding for this project, as well as a GCSSEPM Ed Picou research grant to CML, which funded data collection at Wagon Mound, NM.

CITATIONS

Armstrong, R.L., 1968. The Sevier orogenic belt in Nevada and Utah. Geological Society of America Bulletin 79, 429—458

Arthur, M.A., Schlanger, S.O., and Jenkyns, H.C., 1987. The Cenomanian-Turonian Oceanic Anoxic Event, II. Palaeoceanographic controls on organic-matter production and preservation, *in* J. Brooks and A.J. Fleet, eds., *Marine Petroleum Source Rocks*, *Geological Society Special Publication* 26, p. 401–420.

Arthur, M.A. and Sageman, B.B., 1994. Marine black shales: Depositional mechanisms and environments of ancient deposits: *Annual Reviews of Earth and Planetary Science* v. 22, p. 499-551.

Arthur, M.A. and Sageman, B.B., 2005. Sea-level control on source-rock development: perspectives from the Holocene Black Sea, the mid-Cretaceous Western Interior Basin of North America, and the Late Devonian Appalachian Basin, in: Harris, N.B. (Ed.): *The Deposition of Organic-Carbon-Rich Sediments: Models, Mechanisms and Consequences.* Society for Sedimentary Geology, SEPM Special Publication No. 82, p. 35-59.

765 Arthur, M.A., and Schlanger, S.O., 1979. Cretaceous “Oceanic Anoxic Events” as causal factors in
766 development of reef-reservoired giant oil fields: *American Association of Petroleum Geologists*
767 *Bulletin* v. 63, p. 870-885.

768 Barclay, R.S., McElwain, J.C., and B.B. Sageman, B.B., 2010, Carbon sequestration active by volcanic CO_2
769 pulse during Oceanic Anoxic Event 2, *Nature Geoscience*, v. 3, p. 205–208.
770 doi:10.1038/NGEO757.

771 Barron, E.J., Arthur, M.A., and Kauffman, E.G., 1985, Cretaceous rhythmic bedding sequences: a
772 plausible link between orbital variations and climate: *Earth and Planetary Science Letters* v. 72,
773 p. 327-340.

774 Berger, W.H., Bonneau, M.C., and Parker, F.L., 1982. Foraminifera on the deep-sea floor: lysocline and
775 dissolution rate: *Oceanologica Acta* v. 5, p. 249-258.

776 Bernhard, J.M., 2003, Potential symbionts in Bathyal Foraminifera: *Science* v. 299 p. 861.

777 Blakey, R., 2016. https://deeptimemaps.com/western-interior-seaway-thumbnails/ (accessed 11.5.16).

778 Caldwell, W.G.E., Diner, R., Eicher, D.L., Fowler, S.P., North, B.R., Stelck, C.R., and von Holdt Wilhelm, L.,
779 1993. Foraminiferal Biostratigraphy of Cretaceous Marine Cyclothems, in: Caldwell, W.G.E.,
780 Kauffman, E.G. (Eds.): *Evolution of the Western Interior Basin.* Geological Association of Canada
781 Special Paper 39, p. 477-520

782 Cobban, W.A. and Reeside, J.B., 1952. Frontier Formation, Wyoming and adjacent areas: *American*
783 *Association of Petroleum Geologists Bulletin* v. 36, p. 1913-1961.

784 Corbett, M.J., Watkins, D.K., 2013, Calcareous nannofossil paleoecology of the mid-Cretaceous Western
785 Interior Seaway and evidence of oligotrophic surface waters during OAE2: *Palaeogeography,*
786 *Palaeoclimatology, Palaeoecology* 392, p. 510—523

787 Corbett, M.J., Watkins, D.K., and Popspichal, J.J., 2014. A quantitative analysis of calcareous nannofossil
788 bioevents of the Late Cretaceous (Late Cenomanian-Coniacian) Western Interior Seaway and
789 their reliability in established zonation schemes: *Marine Micropaleontology* v. 109, p. 30-45.

790 Culver, S.J., 1988. New foraminiferal depth zonation of the northwestern Gulf of Mexico: *Palaios* v. 3, p.
791 69—85

792 Da Gama, R.O.B.P., Lutz, B., Desjardins, P., Thompson, M., Prince, and I., Espejo, I., 2014. Integrated
793 paleoenvironmental analysis of the Niobrara Formation: Cretaceous Western Interior Seaway,
794 northern Colorado: *Palaeogeography, Palaeoclimatology, Palaeoecology* v. 413, p. 66-80.

795 Dean, W.E., and Arthur, M.A., 1998. Geochemical expressions of cyclicity in Cretaceous pelagic
796 limestone sequences: Niobrara Formation, Western Interior Seaway, in: Dean, W.E., Arthur,
797 M.A., (Eds.) 1998. *Stratigraphy and Paleoenvironments of the Cretaceous Western Interior*
798 *Seaway, USA*: SEPM Concepts in Sedimentology and Paleontology v. 6, p. 227-255.

799 Denne, R.A., Hinote, R.E., Breyer, J.A., Kosanke, T.H., Lees, J.A., Engelhardt-Moore, N., Spaw, J.M., and
800 Tur, N., 2014. The Cenomanian-Turonian Eagle Ford Group of south Texas: Insights on timing
801 and paleoceanographic conditions from geochemistry and micropaleontologic analyses:
802 *Palaeogeography, Palaeoclimatology, Palaeoecology* v. 413, p. 2-28.

803 Diaz, R.J. and Rosenberg, R., 2008, Spreading dead zones and consequences for marine ecosystems:
804 *Science* v. 321 p. 926-929, doi: 10.1126/science.1156401.

805 Eicher, D.L., 1965. Foraminifera and biostratigraphy of the Graneros Shale: *Journal of Paleontology* v. 39,
806 p. 875-909.

807 Eicher, D.L., 1966. Foraminifera from the Cretaceous Carlile Shale of Colorado: Contributions to the
808 Cushman Foundation for Foraminiferal Research v. 17, p. 16-31.

809 Eicher, D.L., 1967. Foraminifera from Belle Fourche Shale and equivalents, Wyoming and Montana:
810 *Journal of Paleontology* v. 41, p. 167-188.

811 Eicher, D.L. and Worstell, P., 1970. Cenomanian and Turonian foraminifera from the Great Plains, United
812 States: *Micropaleontology* v. 16, p. 269-324.

813 Eicher, D.L. and Diner, R., 1985. Foraminifera as indicators of water mass in the Cretaceous Greenhorn
814 Sea, Western Interior, in: Pratt, L., Kauffman, E.G., Zelt, F.B. (Eds.), *Fine-grained Deposits and*
815 *Biofacies of the Cretaceous Western Interior Seaway: Evidence of Cyclic Depositional Processes*:
816 SEPM Annual Mid-Year Meeting, Field Trip No. 4, 122—134.

817 Eicher, D.L. and Diner, R., 1989. Origin of the Cretaceous Bridge Creek cycles in the Western Interior,
818 United States: *Palaeogeography, Palaeoclimatology, Palaeoecology* v. 74, p. 127-146.

819 Elder, W.P., Gustason, E.R., and Sageman, B.B., 1994. Correlation of basinal carbonate cycles to
820 nearshore parasequences in the Late Cretaceous Greenhorn seaway, Western Interior U.S.A.:
821 *Geological Society of America Bulletin* v. 106, p. 892-902.

822 Elderbak, K., Leckie, R.M., and Tibert, N.E., 2014. Paleoenvironmental and paleoceanographic changes
823 across the Cenomanian-Turonian Boundary Event (Oceanic Anoxic Event 2) as indicated by
824 foraminiferal assemblages from the eastern margin of the Cretaceous Western Interior Seaway:
825 *Palaeogeography, Palaeoclimatology, Palaeoecology* v. 413, p. 29-48 doi:
826 10.1016/j.palaeo.2014.07.002.

827 Elderbak, K. and Leckie, R.M., 2016. Paleocirculation and foraminiferal assemblages of the Cenomanian-
828 Turonian Bridge Creek Limestone bedding couplets: Productivity vs. dilution during OAE2:
829 *Cretaceous Research* v. 60, p. 52-77.

Erbacher, J., Mosher, D., Malone, M., and ODP Leg 207 Scientific Party, 2004. Drilling probes past carbon cycle pertubations on the Demerara Rise: *EOS* v. 85, p. 57-68.

Erbacher, J., Friedrich, O., Wilson, P.A., Birch, H., and Mutterlose, J., 2005. Stable organic carbon isotope stratigraphy across Oceanic Anoxic Event 2 of Demerara Rise, western tropical Atlantic: *Geochemistry, Geophysics, Geosystems* v. 6, Q06010, doi:10.1029/2004GC000850.

Fischer, A.G., Bottjer, D.J., 1991. Orbital forcing and sedimentary sequences: *Journal of Sedimentology and Petrology* v. 61, p. 1063—1069

Fisher, C.G., Kauffman, E.G., and Von Holdt Wilhem, L., 1985. The Niobrara transgressive hemicyclothem in central and eastern Colorado: The anatomy of a multiple disconformity in: Pratt, L., Kauffman, E.G., Zelt, F.B. (Eds.), *Fine-grained Deposits and Biofacies of the Cretaceous Western Interior Seaway: Evidence of Cyclic Depositional Processes*: SEPM Annual Mid-Year Meeting, Field Trip No. 4 p. 184-198.

Fisher, C.G., Hay, W.W., and Eicher, D.L., 1994. Oceanic front in the Greenhorn Sea (late middle through late Cenomanian): *Paleoceanography* v. 9, p. 879-892.

Fisher, C.G., and Arthur, M.A., 2002. Water mass characteristics in the Cenomanian US Western Interior seaway as indicated by stable isotopes of calcareous organisms: *Palaeogeography, Palaeoclimatology, Palaeoecology* v. 188, p. 189-213.

Floegel, S., Hay, W.W., DeConto, R.M., and Balukhovsky, A.N., 2005. Formation of sedimentary bedding couplets in the Western Interior Seaway of North America—implications from climate system modeling: *Palaeogeography, Palaeoclimatology, Palaeoecology* v. 218, p. 125-143.

Frerichs, W.E., 1979. Planktonic Foraminifera from the Sage Breaks Shale, Centennial Valley, Wyoming: *Journal of Foraminiferal Research* v. 9, p. 159-184.

852 Frerichs, W.E., and Gaskill, C., 1988. Planktic foraminifera and the age of the Niobrara in its type area:
853 *Contributions to Geology, University of Wyoming* v. 26, p. 5-13.

854 Frush, M.P., and Eicher, D.L., 1975. Cenomanian and Turonian foraminifera and paleoenvironments in
855 the Big Bend region of Texas and Mexico, in: Caldwell, W.G.E. (Ed.), *The Cretaceous System in*
856 *the Western Interior of North America*: The Geological Society of Canada Special Paper 13, p.
857 277—301.

858 Gilbert, G.K., 1895. Sedimentary measurement of geologic time: *Journal of Geology* v. 3, p. 121-127.

859 Gooday, A.J., 2003. Benthic Foraminifera (Protista) as tools in deep-water palaeoceanography:
860 environmental influences on faunal characteristics: *Advances in Marine Biology* v. 46, p. 1-90

861 Gurnis, M., 1993. Phanerozoic marine inundation of continents driven by dynamic topography above
862 subducting slabs: *Nature* v. 364, p. 589-593

863 Hancock, J.M., and Kauffman, E.G., 1979. The great transgressions of the Late Cretaceous: *Journal of the*
864 *Geological Society of London* v. 136, p. 175-186.

865 Hartnett, H.E., Keil, R.G., Hedges, J.I. and Devol, A.H., 1998. Influence of oxygen exposure time on
866 organic carbon preservation in continental margin sediments, *Nature* v. 391, p. 572-575
867 doi:10.1038/35351.

868 Hattin, D.E., 1975. Petrology and origin of fecal pellets in Upper Cretaceous strata of Kansas and
869 Sakatchewan: *Journal of Sedimentary Petrology* v. 45, p. 686-696

870 Hattin, D.E. and Cobban, W.A., 1977. Fourth and fifth days: Upper Cretaceous stratigraphy, paleontology
871 and paleoecology of western Kansas: *The Mountain Geologist* v. 14, p. 175-215.

872 Hattin, D.E., 1982. Stratigraphy and depositional environment of Smoky Hill Chalk Member, Niobrara
873 Chalk (Upper Cretaceous) of the type area, western Kansas: *Bulletin-Kansas State Geological*
874 *Survey*, v. 225, 108 pp.

875 Hattin, D.E., 1986. Carbonate substrates of the Late Cretaceous Sea, central Great Plains and southern
876 Rocky Mountains: *Palaios*, v. 1, p. 347-367.

877 Hay, W.W., Eicher, D.L., and Diner, R., 1993. Physical oceanography and water masses in the Cretaceous
878 Western Interior Seaway, in: Caldwell, W.G.E., and Kauffman, E.G. (Eds.), *Evolution of the*
879 *Cretaceous Western Interior Basin*: Geological Association of Canada Special Paper 39, p. 297-
880 318.

881 Helly, J.J. and Levin, L.A., 2004. Global distribution of naturally occurring marine hypoxia on continental
882 margins: *Deep-Sea Research Part I*, v. 51 p. 1159-1168, doi:10.1016/j.dsr.2004.03.009

883 Ito, T., Minobe, S., Long, M.C., and Duetsch, C., 2017. Upper ocean O_2 trends: 1958-2015: *Geophysical*
884 *Research Letters* v. 44, p. 4214-4223 doi:10.1002/2017GL073613.

885 Jenkyns, H.C., 2010. Geochemistry of oceanic anoxic events: *Geochemistry Geophysics Geosystems* v. 11,
886 Q03004, doi:10.1029/2009GC002788.

887 Joo, Y.I., Sageman, B.B., 2014. Cenomanian to Campanian carbon isotope chemostratigraphy from the
888 Western Interior Basin, U.S.A: *Journal of Sedimentary Research*, v. 84, p. 529-542

889 Jorissen, F.J., de Stigter, H.C., and Widmark, J.G.V. (1995), A conceptual model explaining benthic
890 foraminiferal microhabitats, *Marine Micropaleontology*, v. 26, p. 3–15.

891 Jorissen, F.J., Fontanier, C., and Thomas, E., 2007. Paleoceanographical proxies based on deep-sea
892 benthic foraminiferal assemblage characteristics: *Developments in Marine Geology* v. 1, p. 263-
893 325 doi:10.1016/S1572-5480(07)01012-3

894 Kauffman, E.G., 1969. Cretaceous marine cycles of the Western Interior: *The Mountain Geologist* v. 6, p.
895 227-245.

896 Kauffman, E.G., 1977. Geological and biological overview: Western Interior Cretaceous Basin, in:
897 Kauffman, E.G. (Ed.), Cretaceous facies, faunas and paleoenvironments across the Western
898 Interior Basin: *Mountain Geologist* v. 14, p. 75-99

899 Kauffman, E.G., 1984. Paleobiogeography and evolutionary response dynamic in the Cretaceous
900 Western Interior Seaway of North America, in: Westermann, G.E.G. (Ed.), *Jurassic-Cretaceous*
901 *Biochronology and Paleogeography of North America*: Geological Association of Canada Special
902 Paper 27, p. 273-306.

903 Kauffman, E.G., Caldwell, W.G.E., 1993. The Western Interior Basin in space and time. in: Kauffman, E.G.
904 Caldwell, W.G.E. (Ed.), Evolution of the Western Interior Basin: *Geological Association of Canada*
905 *Special Paper* v. 39, p. 1-30

906 Kent, H.C., 1968. Biostratigraphy of Niobrara-equivalent part of Mancos Shale (Cretaceous) in
907 northwestern Colorado: *American Association of Petroleum Geologists Bulletin* v. 52, p. 2098—
908 2115

909 Kita, Z.A., Watkins, D.K., and Sageman, B.B., 2017. High-resolution calcareous nannofossils
910 biostratigraphy of the Santonian/Campanian Stage boundary, Western Interior Basin, USA:
911 *Cretaceous Research* v. 69, p. 49-55. http://dx.doi.org/10.1016/j.cretres.2016.08.015.

912 Kominz, M.A., Browning, J.V., Miller, K.G., Sugarman, P.J., Mizintseva, S., and Scotese, C.R., 2008. Late
913 Cretaceous to Miocene sea-level estimates from the New Jersey and Delaware coastal plain
914 boreholes: an error analysis: *Basin Research* v. 20, p. 211-226 doi: 10.1111/j.1365-
915 2117.2008.00354.x

916 Kump, L.R. and Slingerland, R.L., 1999. Circulation and stratification of the early Turonian Western
917 Interior Seaway: Sensitivity to a variety of forcings, in: Barrera, E., Johnson, C. (Eds.), *Evolution of*
918 *Cretaceous Ocean-Climate System*: Geological Society of America Special Paper 332, p. 93-104.

919 Kuypers, M.M.M., Pancost, R.D., Nijenhuis, I.A., and Sinninghe Damsté, J.S., 2002. Enhanced productivity
920 led to increased organic carbon burial in the euxinic North Atlantic basin during the late
921 Cenomanian oceanic anoxic event: *Paleoceanography* v. 17, doi:10.1029/2000PA000569.

922 Laferriere, A.P., 1992. Regional isotopic variations in the Fort Hays Member of the Niobrara Formation,
923 United States Western Interior: Primary signals and diagenetic overprinting in a Cretaceous
924 pelagic rhythmite: *Geological Society of America Bulletin* v. 104, p. 980-992.

925 Larson, R.L., 1991a. Latest pulse of Earth: Evidence for a mid-Cretaceous superplume: *Geology* v. 19, p.
926 547-550.

927 Larson, R.L., 1991b. Geologic consequences of superplumes: *Geology* v. 19, p. 963-966.

928 Leckie, R.M., Kirkland, J.I., and Elder, W.P., 1997. Stratigraphic framework and correlation of a principal
929 reference section of the Mancos Shale (Upper Cretaceous), Mesa Verde, Colorado, in: Anderson,
930 O., Kues, B., and Lucas, S. (Eds.), *Mesozoic Geology and Paleontology of the Four Corners Region*:
931 New Mexico Geological Society Guidebook, 48th Field Conference, p. 163-216.

932 Leckie, R.M., Yuretich, R.F., West, O.L.O, Finkelstein, D., and Schmidt, M., 1998. Paleoceanography of the
933 southwestern Western Interior Sea during the time of the Cenomanian-Turonian boundary (Late
934 Cretaceous), in: Dean, W.E., and Arthur, M.A. (Eds.), *Stratigraphy and Paleoenvironments of the*
935 *Cretaceous Western Interior Seaway, U.S.A*: SEPM Concepts in Sedimentology and Paleontology
936 6, p. 101-126.

Leckie, R.M., Bralower, T.J., and Cashman, R. (2002), Oceanic anoxic events and plankton evolution: biotic response to tectonic forcing during the mid-Cretaceous*, Paleoceanography*, v. 17, 10.1029/2001PA000623.

Leckie, R.M., and Olson, H.C. (2003), Foraminifera as proxies for sea-level change on siliciclastic margins, in: Olson, H.C., and R.M. Leckie, eds., Micropaleontologic proxies for sea-level change and stratigraphic discontinuities, *SEPM Special Publication* No. 75, p. 5–19.

Liu, S.F., Nummendal, D., and Gurnis, M., 2014. Dynamic versus flexural controls of Late Cretaceous Western Interior Basin, USA: *Earth and Planetary Science Letters* v. 389, p. 221—229.

Liu, S.F., Nummendal, D., 2004. Late Cretaceous subsidence in Wyoming: Quantifying the dynamic component: *Geology* v. 32, p. 397-400

Liu, S.F., Nummendal, D., Yin, P.G., Huo, H.J., 2005. Linkage of Sevier thrust episodes and Late Cretaceous megasequences across southern Wyoming (USA): *Basin Research* v. 17, p. 487-506

Liu, S.F., Spasojevic, S., Gurnis, M., 2008. Reconstructing Farallon plate subduction beneath North America back to the Late Cretaceous: *Science* v. 322, p. 934-938

Liu, S.F., Nummendal, D., Liu, L.J., 2011. Migration of dynamic subsidence across the Late Cretaceous United States Western Interior Basin in response to Farallon plate subduction: *Geology* v. 39, p. 555-558

Locklair, R., and Sageman, B.B., 2008. Cyclostratigraphy of the Upper Cretaceous Niobrara Formation, Western Interior, U.S.A.: A Coniacian-Santonian orbital timescale: *Earth and Planetary Science Letters* v. 269, p. 540-553.

957 Locklair, R., Sageman, B.B., and Lerman, A., 2011. Marine carbon burial flux and the carbon isotope
958 record of Late Cretaceous (Coniacian–Santonian) Oceanic Anoxic Event III: *Sedimentary Geology*
959 v. 235, p. 38-49.

960 Lockshin, S. Yacobucci, M.M., Gorsevski, P., and Gregory, A., 2017. Spatial characterization of Cretaceous
961 Western Interior Seaway paleoceanography using foraminifera, fuzzy sets and Dempster-Shafer
962 theory: *GeoResJ*, doi: 10.1016/j.grj.2017.10.001.

963 Longman, M.W., Luneau, B.A., and Landon, S.M., 1998. Nature and distribution of Niobrara lithologies in
964 the Cretaceous Western Interior Seaway of the Rocky Mountain Region: *The Mountain Geologist*
965 v. 35, p. 137—170.

966 Lowery, C.M., Corbett, M.J., Leckie, R.M., Watkins, D., Staerker, T.S., Donovan, A.D., Miceli Romero, A.,
967 Pramudito, A., 2014. Foraminiferal and nannofossil paleoecology and paleoceanography and the
968 Cenomanian-Turonian Eagle Ford Shale across southern Texas: *Palaeogeography,*
969 *Palaeoclimatology, Palaeoecology* v. 413, p. 49-65
970 http://dx.doi.org/10.1016/j.palaeo.2014.07.025.

971 Lowery, C.M., Leckie, R.M., and Sageman, B.B., 2017. Micropaleontological evidence for redox changes
972 in the OAE3 interval of the US Western Interior: Global vs. local processes: *Cretaceous Research*
973 v. 69, p. 34-48, http://dx.doi.org/10.1016/j.cretres.2016.08.011.

974 Ma, C., Meyers, S.R., Sageman, B.B., Singer, B.S., Jicha, B.R., 2014. Testing the astronomical time scale
975 for oceanic anoxic event 2, and its extension into the Cenomanian strata of the Western Interior
976 Basin (USA): *Geological Society of America Bulletin* v. 126, 974-989.

977 McGookey, D.P., Haun, J.D., Hale, L.A., McCubbin, D.G., Weimer, R.J., Wolf, G.R., 1972. Cretaceous
978 system, in: Mallory, W.W. (Ed.), Geologic Atlas of the Rocky Mountain Region, U.S.A., Rocky
979 Mountain Association of Geologists, Denver, CO, p. 190-228

980 McNeil, D.H., Caldwell, W.G.E., 1981. Cretaceous rocks and their foraminifera in the Manitoba
981 escarpment, Geological Association of Canada Special Paper 21

982 Merewether, E.A., Cobban, W.A., and Obradovich J.D., 2011. Biostratigraphic data from Upper
983 Cretaceous formations—eastern Wyoming, central Colorado, and northeastern New Mexico: *US*
984 *Geologic Survey Scientific Investigations Map* 3175, 2 sheets, 10 p.

985 Meyers, S., Sageman, B.B., Hinnov, L., 2001. Integrated quantitative stratigraphy of Cenomanian-
986 Turonian Bridge Creek Limestone Member using evolutive harmonic analysis and stratigraphic
987 modeling: *Journal of Sedimentary Research* v. 71, p. 628-644

988 Meyers, S.R., Sageman, B.B., Lyons, T.W., 2005. Organic carbon burial rate and the molybdenum proxy:
989 theoretical framework and application to Cenomanian-Turonian Oceanic Anoxic Event 2:
990 *Paleoceanography* v. 20, PA2002, doi:10.1029/2004PA001068

991 Meyers, S.R., Sageman, B.B., and Arthur, M.A., 2012. Obliquity forcing of organic matter accumulation
992 during Oceanic Anoxic Event 2: *Paleoceanography* v. 27, doi:10.1029/2012PA002286

993 Molenaar, C.M., 1983. A principal reference section and correlation of the Gallup Sandstone,
994 northwestern New Mexico, in: Hook, S.C. (Ed.), Contributions to mid-Cretaceous paleontology
995 and stratigraphy of New Mexico—Part II: *New Mexico Bureau of Mines and Mineral Resources*
996 *Circular* 185, p. 29-40

997 Molenaar, C.M., Cobban, W.A., Mereweather, E.A., Pillmore, C.L., Wolfe, D.G., and Holbrook, J.M., 2002.
998 Regional stratigraphic cross sections of Cretaceous rocks from east-central Arizona to the
999 Oklahoma panhandle: *USGS Miscellaneous Field Studies Map* MF-2382.

1000 Monteiro, F.M., R.D. Pancost, A. Ridgwell, and Y. Donnadieu (2012), Nutrients as the dominant control
1001 on the spread of anoxia and euxinia across the Cenomanian-Turonian oceanic anoxic event
1002 (OAE2): Model-data comparison: *Paleoceanography* v. 27, PA4209. doi: 10.1029/2012PA002351.

1003 Müller, R.D., M. Sdrolias, C. Gaina, and W.R. Roest (2008), Age, spreading rates, and spreading
1004 asymmetry of the world's ocean crust: *Geochemistry, Geophysics, Geosystems* v. 9, Q04006,
1005 doi:10.1029/1007GC001743.

1006 Nielsen, K.S., Schröder-Adams, C., Leckie, D.A., Haggart, J.W., and Elberdak, K., 2008. Turonian to
1007 Santonian paleoenvironmental changes in the Cretaceous Western Interior Sea: The Carlile and
1008 Niobrara formations in southern Alberta and southwestern Saskatchewan, Canada:
1009 *Palaeogeography, Palaeoclimatology, Palaeoecology*, v. 270, p. 64-91.

1010 Oschlies, A., Schultz, K.G., Riesbesell, U., Schmittner, A., 2008. Simulated 21 century's increase in oceanic
1011 suboxia in CO_2-enhanced biotic carbon export: *Global Biogeochemical Cycles* v. 22,
1012 doi:10.1029/2007GB003147

1013 Pang, M., Nummendal, D., 1995. Flexural subsidence and basement tectonics of the Cretaceous Western
1014 Interior Basin, United States: *Geology* v. 23, p. 173-176

1015 Poag, C.W. (1981), *Ecological Atlas of Benthic Foraminifera of the Gulf of Mexico*: Marine Science
1016 International, Woods Hole, MA, 174 p.

1017 Pogge von Strandmann, P.A.E., H.C. Jenykyns, and R.G. Woodfine, (2013). Lithium isotope evidence for
1018 enhanced weathering during Oceanic Anoxic Event 2: *Nature Geoscience* v. 6, p. 668–672, doi:
1019 10.1038/NGEO1875

1020 Pratt, L.M., and Threlkeld, C.N., 1984. Stratigraphic significance of $^{13}C/^{12}C$ ratios in mid-Cretaceous rocks
1021 of the Western Interior, U.S.A., in: Stott, D.F., Glass, D.J. (Eds.), *The Mesozoic of Middle North*
1022 *America*: Canadian Society of Petroleum Geologists Memoir 9, p. 305-312.

1023 Pratt, L.M., Arthur, M.A., Dean, W.E., and Scholle, P.A., 1993. Paleo-oceanographic cycles and events
1024 during the Late Cretaceous in the Western Interior Seaway of North America, in: Caldwell,
1025 W.G.E. and Kauffman, E.G., (Eds.), *The Evolution of the Western Interior Basin: Geological Society*
1026 *of Canada Special Paper* 39, p. 333-353.

1027 Rabalais, N.N. and Turner, R.E., Eds., 2001. *Coastal Hypoxia: Consequences for Living Resources and*
1028 *Ecosystems*, American Geophysical Union, Washington, DC.

1029 Ryer, T.A. and Lovekin, J.R., 1986. The Upper Cretaceous Vernal Delta of Utah – Depositional or
1030 paleotectonic feature? In: Peterson, J.A., (Ed.), Paleotectonics and Sedimentation in the Rocky
1031 Mountain Region: *America Association of Petroleum Geologists Memoir* 41, p. 497-510.

1032 Sageman, B.B., 1996. Lowstand tempestites: Depositional model for Cretaceous skeletal limestones,
1033 Western Interior Basin: *Geology*, v. 24, p. 888-892.

1034 Sageman, B.B. and Lyons, T.W., 2003. Geochemistry of fine-grained sediments and sedimentary rocks, in
1035 Mackenzie, F., Ed., *Treatise on Geochemistry*, Elsevier, Oxford, p. 115-158.

1036 Sageman, B.B., Singer, B.S., Meyers, S.R., Siewert, S.E., Walaszczyk, I., Condon, D.J., Jicha, B.R.,
1037 Obradovich, J.D., and Sawyer, D.A., 2014. Integrating $^{40}Ar/^{39}Ar$, U-Pb, and astronomical clocks in
1038 the Cretaceous Niobrara Formation, Western Interior Basin, USA: *Geological Society of America*
1039 *Bulletin* v. 126, p. 956-973.

1040 Schlanger, S.O., Jenkyns, H.C. 1976. Cretaceous oceanic anoxic events: causes and consequences:
1041 *Geologie En Mijnbouw* v. 55, p. 179-184

1042 Schlanger, S.O., Arthur, M.A., Jenkyns, H.C., and Cholle, P.A., 1987. The Cenomanian-Turonian Oceanic
1043 Anoxic Evnet, I. Stratigraphy and distribution of organic carbon-rich beds and the marine d13C
1044 excursion, in: Brooks, J. and Fleet, A.J., (Eds.), Marine Petroleum Source Rocks: *Geological*
1045 *Society Special Publication* 26, p. 371-399.

1046 Scholle P.A. and M.A. Arthur (1980), Carbon isotope fluctuations in Cretaceous pelagic limestones:
1047 potential stratigraphic and petroleum exploration tool: *American Society of Petroleum*
1048 *Geologists Bulletin* v. 64, p. 67–87.

1049 Schröder-Adams, C.J., Herrle, J.O., Embry, A.F., Haggart, J.W., Galloway, J.M., Pugh, A.T., and Harwood,
1050 D.M., 2014. Aptian to Santonian foraminifera biostratigraphy and paleoenvironmental change in
1051 the Sverdrup Basin as revealed at Glacier Fiord, Axel Heiberg Island, Canadian Arctic
1052 Archipelago: *Palaeogeography, Palaeoclimatology, Palaeoecology* v. 413, p. 81-100, doi:
1053 10.1016/j.palaeo.2014.03.010.

1054 Schwatrz, R.K. and DeCelles, P.G., 1988. Cordilleran Foreland Basin evolution in response to interactive
1055 Cretaceous thrusting and foreland partitioning, southwestern Montana: *Geological Society of*
1056 *America Memoir 171*, 61 p.

1057 Scott, G.R., and Cobban, W.A., 1964. Stratigraphy of the Niobrara Formation at Pueblo, Colorado: *U.S.*
1058 *Geological Survey Professional Paper*, Report P 0454-L, p. L1-L30.

1059 Scott, G.R., Cobban, W.A., and Merewether, E.A., 1986. Stratigraphy of the Upper Cretaceous Niobrara
1060 Formation in the Raton Basin, New Mexico: New Mexico Bureau of Mines and Mineral
1061 Resources Bulletin 115, 36 p.

1062 Sikora, P.J., Howe, R.W., Gale, A.S., and Stein, J.A., 2004. Chronostratiography of proposed Turonian-
1063 Coniacian (Upper Cretaceous) stage boundary stratotypes: Salzgitter-Salder, Germany, and
1064 Wagon Mound, New Mexico, USA, in: Beaudoin, A.B., and Head, M.J. (Eds.), The Palynology and

Micropalaeontology of Boundaries: Geological Society, London, Special Publication 230, p. 207-242.

Slingerland, R., Kump, L.R., Arthur, M.A., Fawcett, P.J., Sageman, B.B., and Barron, E.J., 1996. Estuarine circulation in the Turonian Western Interior Seaway of North America: *Geological Society of America Bulletin* v. 108, p. 941-952.

Snow, L.J., Duncan, R.A., Bralower, T.J., 2005. Trace element abundances in the Rock Canyon Anticline, Pueblo, Colorado, marine sedimentary section and their relationship to Caribbean plateau construction and Oxygen Anoxic Event 2: *Paleoceanography* v. 20, PA3005, doi:10.1029/2004PA001093

Stramma, L., Schmidt, S., Levin, L.A., and Johnson, G.C., 2010. Ocean oxygen minima expansions of their biological impacts: *Deep Sea Research I* v. 57, p. 587-595.

Svarda, C.E., 1998a. Ichnology of the Bridge Creek Limestone: Evidence for temporal and spatial variations in paleo-oxygenation in the Western Interior Seaway, in: Dean, W.E., and Arthur, M.A., (Eds.) *Stratigraphy and paleoenvironments of the Cretaceous Western Interior Seaway, USA,* SEPM Concepts in Sedimentology and Paleontology 6, p. 127–136.

Svarda, C.E., 1998b. Ichnocoenoses in the Niobrara Formation: Implications for benthic oxygenation histories, in: Dean, W.E., Arthur, M.A. (Eds.), *Stratigraphy and Paleoenvironments of the Cretaceous Western Interior Seaway, U.S.A*: SEPM Concepts in Sedimentology and Paleontology 6, p. 137-151.

Trabucho-Alexandre, J., Negri, A., de Boer, P.L., 2011. Early Turonian pelagic sedimentation at Moria (Umbria-Marche, Italy): Primary and diagenetic controls on lithological oscillations: *Palaeogeography, Palaeoclimatology, Palaeoecology* v. 311, p. 200-214

1087 Tessin, A., Hendy, I., Sheldon, N., and Sageman, B., 2015. Redox-controlled preservation of organic
1088 matter during “OAE3” within the Western Interior Seaway: *Paleoceanography* v. 30,
1089 doi:10.1002/2014PA002729.tsi.

1090 Tessin, A., Sheldon, N.D., Hendy, I., and Chappaz, A., 2016. Iron limitation in the Western Interior
1091 Seaway during the Late Cretaceous OAE 3 and its role in phosphorus cycling and enhanced
1092 organic matter preservation: *Earth and Planetary Science Letters* v. 449, p. 135-144. doi:
1093 10.1016/j.epsl.2016.05.043

1094 Tibert, N.E., R.M. Leckie, J.G. Eaton, J.I. Kirkland, J.P. Colin, E.L. Leithold, and Michael E. McCormic
1095 (2003), Recognition of relative sea-level change in Upper Cretaceous coal-bearing strata: A
1096 paleoecological approach using agglutinated foraminifera and ostracodes to detect key
1097 stratigraphic surfaces, in: H.C. Olson, and Leckie, R.M. (Eds.), *Micropaleontologic proxies for sea-*
1098 *level change and stratigraphic discontinuities, Society of Economic Paleontologists and*
1099 *Mineralogists Special Publication* 75, p. 263–299

1100 Tibert, N.E. and Leckie, R.M., 2004. High-resolution estuarine sea level cycles from the Late Cretaceous:
1101 Amplitude constraints using agglutinated foraminifera: *Journal of Foraminiferal Research* v. 34,
1102 p. 130-143.

1103 Tibert, N.E. and Leckie, R.M., 2013. Cenomanian-Turonian foraminfera from the westernmost Colorado
1104 Plateau: *Micropaleontology* v. 59, p. 1-24.

1105 Tsikos, H., Jenkyns, H.C., Walsworth-Bell, B., Petrizzo, M.R., Forster, A., Kolonic, S., Erba, E., Premoli Silva,
1106 I., Baas, M., Wagner, T., and Sinninghe Damsté, J.S., 2004. Carbon-isotope stratigraphy recorded
1107 by the Cenomanian-Turonian oceanic anoxic event: Correlation and implications based on three
1108 key localities: *Journal of the Geological Society of London* v. 161, p. 711-720.

1109 Van Bentum, E.C., Reichart, G.-J., Forster, A., and Sinnighe Damsté, J.S. 2012, Latiudinal differences in
1110 the amplitude of the OAE-2 carbon isotope excursion: pCO_2 and paleo productivity:
1111 *Biogeosciences*, v. 9, p. 717–731. doi:10.5194/bg-9-717-2012.

1112 Van der Zwaan, G.J., Jorissen, F.J., and Stitger, H.C., 1990, The depth dependency of planktonic/benthic
1113 foraminiferal ratios: constraints and applications: *Marine Geology*, v. 95, p. 1–16.

1114 Van Hinsbergen, D.J.J., T.J. Kouwenhoven, and G.J. Van der Zwaan (2005), Paleobathymetry in the
1115 backstripping procedure: correction of oxygenation effects on depth estimates,
1116 *Palaeogeography, Palaeoclimatology, Palaeoceology*, 21, 245–265.

1117 Villien, A., and Kligfield, R.M., 1986. Thrusting and synorogenic sedimentation in central Utah: *American*
1118 *Association of Petroleum Geologists Memoir* 41, p. 281-308.

1119 Wagner, T., Sinnighe Damste, J.S., Hotmann, P., Beckmann, B., 2004. Euxinia and primary production in
1120 Late Cretaceous equatorial Atlantic surface waters fostered in orbitally driven formation of
1121 marine black shales: *Paleoceanography* v. 19, PA3009

1122 Wagreich, M., 2009. Coniacian-Santonian oceanic red beds and their link to Oceanic Anoxic Event 3, in:
1123 Hu, X., Wang, C., Scott, R., Wagreich, M., Jansa, L., (Eds.), Cretaceous Oceanic Red Beds:
1124 Stratigraphy, Composition, Origins, and Paleoceanographic and Paleoclimatic Significance: *SEPM*
1125 *Special Publication* 91, p. 235-242

1126 Wagriech, M., 2012. "OAE3" – regional Atlantic organic carbon burial during the Coniacian-Santonian:
1127 *Climate of the Past* v. 8, p. 1447-1455.

1128 Wang, C., Hu, X., 2005. Cretaceous world and oceanic red beds: *Earth Science Frontiers* 2005, p. 11-21

1129 Wang, C.S., Hu, X., Huang, Y., Wagreich, M., Scott, R., Hay, W., 2011. Cretaceous oceanic red beds as
1130 possible consequence of oceanic anoxic events: *Sedimentary Geology* v. 235, 27-37

Watkins, D.E., Bralower, T.J., Covington, J.M., and Fisher, C.G., 1993. Biostratigraphy and paleoecology of the Upper Cretaceous calcareous nannofossils in the Western Interior Basin, North America, in: Caldwell, W.G.E., and Kauffman, E.G. (Eds.), *Evolution of the Western Interior Basin*: Geological Association of Canada Special Paper 39, p. 521-537.

Weimer, R.J., 1978, Influence of Transcontinental Arch on Cretaceous marine sedimentation – a preliminary report, in: Pruitt, J.D. and Coffin, P.E. (Eds.), Energy Resources of the Denver Basin, *Rocky Mountain Association of Geologists 1978 Symposium* p. 111-222.

West, O.L.O., Leckie, R.M., and Schmidt, M., 1998. Foraminiferal paleoecology and paleoceanography of the Greenhorn Cycle along the southwestern margin of the Western Interior Sea, in: Dean, W.E., Arthur, M.A. (Eds.), *Stratigraphy and Paleoenvironments of the Cretaceous Western Interior Seaway, U.S.A*: SEPM Concepts in Sedimentology and Paleontology 6, p. 79-99.

White, T., Furlong, K., and Arthur, M., 2002. Forebulge migration in the Cretaceous Western Interior basin of the central United States: *Basin Research* v. 14, p. 43-54.

Wignall, P.B., 1991. Model for transgressive black shales? *Geology* v. 19, p. 167-170.